

Mixed Membership Graph Clustering via Systematic Edge Query

Shahana Ibrahim and Xiao Fu

School of Electrical Engineering and Computer Science
Oregon State University
Corvallis, OR 97331, United States

(ibrahish,xiao.fu)@oregonstate.edu

June 22, 2022

Abstract

This work considers clustering nodes of a largely incomplete graph. Under the problem setting, only a small amount of queries about the edges can be made, but the entire graph is not observable. This problem finds applications in large-scale data clustering using limited annotations, community detection under restricted survey resources, and graph topology inference under hidden/removed node interactions. Prior works treated this problem as a convex optimization-based matrix completion task. However, this line of work is designed for learning *single* cluster membership of nodes belonging to disjoint clusters, yet *mixed* (multiple) cluster membership nodes and overlapping clusters often arise in practice. Existing works also rely on the uniformly random edge query pattern and nuclear norm-based optimization, which give rise to a number of implementation and scalability challenges. This work aims at learning mixed membership of the nodes of overlapping clusters using edge queries. Our method offers membership learning guarantees under *systematic query patterns* (as opposed to random ones). The query patterns can be controlled and adjusted by the system designers to accommodate implementation challenges—e.g., to avoid querying edges that are physically hard to acquire. Our framework also features a lightweight and scalable algorithm. Real-data experiments on crowdclustering and community detection are used to showcase the effectiveness of our method.

1 Introduction

Graph clustering is of broad interest in data science, which aims at associating the nodes of a graph with different clusters in an unsupervised manner [1]. Graph clustering is well-motivated, since network data frequently arise in various applications (e.g., in social network analysis, brain signal processing, and biological/ecological data mining). Graph clustering is also an important technique for nonlinear dimensionality reduction; see, e.g., the graph Laplacian technique widely used in spectral clustering [2, 3].

Graph clustering has been extensively studied in the past two decades [4–9], but some major challenges arise in the era of big data. Notably, many graph data are highly incomplete for various reasons. For example, Facebook and Twitter follower-followee data could easily contain billions of nodes, which translates to $\approx 10^{18}$ edges. Edge acquisition at such a scale is a highly nontrivial

task. In many cases, instead of collecting edge information of the entire network, data analysts have to *sample* edges of interest, and use the sampled network to perform graph clustering and other analytical tasks [10,11]. Note that graph sampling (or edge query)-based network analysis is also well-motivated in many other cases—e.g., in community detection of networks where edges are intentionally removed or hidden (e.g., terrorist networks or radical group networks) [12] and in biological/ecological networks where acquiring the complete edge information is too resource-consuming [13,14].

A number of works have considered the graph clustering problem under incomplete edge observation. Specifically, in [15–17], random edge queries were used to sample the graph, and node membership identification guarantees were established under the assumptions that every node is associated with a single cluster and the node-node adjacency graph is generated following the so-called *stochastic blockmodel* (SBM) [18].

1.1 Challenges

The existing approaches in [15–17] are effective to a certain extent, but a number of challenges remain. First, the theoretical guarantees and algorithms were built upon the SBM, in which all nodes admit single cluster membership and belong to disjoint clusters. However, nodes often admit mixed membership and the clusters are usually overlapped in real-world networks (e.g., a person in a co-author network could belong to the machine learning and statistics communities simultaneously). Second, the edges in existing works were queried randomly, which may not be easy to implement in some applications; e.g., in field survey based network analysis spanning a large geographic area [19], surveys are easier to be conducted within local communities, other than randomly scattered geographically. Random query is also not suitable for handling networks with hidden or intentionally removed edges. Third, the works in [15–17] recast the edge query-based graph clustering problem as a nuclear norm minimization based convex optimization problem, which entails N^2 (where N is the number of nodes) optimization variables—making it hard to scale up for real-world large-scale graphs.

1.2 Contributions

In this work, we offer an alternative framework for learning the node membership from incomplete graph. Some notable features of our framework are as follows:

Systematic Edge Query Strategy Our algorithm design comes with *systematic* edge query patterns, under which the node membership can be provably learned. As discussed, systematic query may be more preferable than random query in a variety of applications.

Mixed Membership Identification Unlike existing provable edge-query based graph clustering methods in [15–17] that only learn single membership of nodes belonging to disjoint clusters, we model the undirected adjacency graphs using a mixed membership model that allows nodes to be associated with multiple overlapping clusters. Accordingly, we offer mixed membership identification guarantees using queried edges.

Scalable and Lightweight Algorithm We propose a simple procedure that only consists of the truncated *singular value decomposition* (SVD) of small matrices and a Gram–Schmidt-type

greedy algorithm for *simplex-structured matrix factorization* (SSMF). This procedure is much more economical compared to the convex optimization approaches in [15–17,20]. We also provide sample complexity and noise robustness analyses for the proposed framework.

Evaluation on Real-World Datasets We conduct extensive evaluation on real-world datasets. First, we consider the query-based crowdclustering task [15, 16], using annotator-labeled graph data to assist image clustering. The data used in our evaluation was uploaded to the *Amazon Mechanical Turk* (AMT) platform and labeled by unknown human annotators. The acquired AMT data has been made publicly available¹. Second, we also use co-authorship network datasets, *Digital Bibliography & Library Project* (DBLP) and *Microsoft Academic Graph* (MAG), to evaluate our method on community detection tasks.

1.3 Prior Conference Submission

An initial and limited version of this work was submitted to IEEE ICASSP 2021 [21]. In this journal version, we additionally include (1) detailed identifiability analysis of the proposed algorithm (Theorem 1 and its proof); (2) the integrated performance characterization of the SVD and SSMF stages (Theorem 2 and its proof); (3) a new application, namely, crowdclustering; (4) a series of new real-data experiments; (5) and a newly acquired dataset for crowdclustering that is made publicly available.

1.4 Notation

$x, \mathbf{x}, \mathbf{X}$ denote a scalar, vector and matrix, respectively. $\kappa(\mathbf{X})$ denotes the condition number of the matrix \mathbf{X} and is given by $\kappa(\mathbf{X}) = \frac{\sigma_{\max}(\mathbf{X})}{\sigma_{\min}(\mathbf{X})}$ where σ_{\max} and σ_{\min} are the largest and smallest nonzero singular values of \mathbf{X} , respectively. $\mathbf{X} \geq \mathbf{0}$ denotes that all the elements of \mathbf{X} are nonnegative. $\|\mathbf{X}\|_2$ represents the 2-norm of matrix \mathbf{X} , i.e., $\|\mathbf{X}\|_2 = \sigma_{\max}(\mathbf{X})$. $\|\mathbf{X}\|_F$ denotes the Frobenius norm of \mathbf{X} . $\text{range}(\mathbf{X})$ denotes the subspace spanned by the columns of \mathbf{X} . $\mathbf{X}(i, j)$ and $x_{i,j}$ both denote the element of \mathbf{X} from its i th row and j th column. $\mathbf{X}(:, j)$ and \mathbf{x}_j both denote the j th column of \mathbf{X} . $\|\mathbf{x}\|_2$ and $\|\mathbf{x}\|_1$ denote ℓ_2 and ℓ_1 norms of vector \mathbf{x} , respectively. \top and \dagger denote transpose and pseudo-inverse, respectively. $|\mathcal{C}|$ denotes the cardinality of set \mathcal{C} . \cup denotes the union operator for sets. $[T]$ represents the set of positive integers up to T , i.e., $[T] = \{1, \dots, T\}$. $\text{Diag}(\mathbf{x})$ is a diagonal matrix that holds the entries of \mathbf{x} as its diagonal elements.

2 Problem Statement

Consider N data entities (e.g., persons in a social network or image data in a sample-sample similarity network) that are from K clusters. We allow a node to belong to multiple clusters; i.e., we consider the case where the clusters have overlaps and the nodes admits *mixed membership*. Assume that the n th entity belongs to cluster k with probability $m_{k,n}$, where

$$\sum_{k=1}^K m_{k,n} = 1, \quad m_{k,n} \geq 0. \quad (1)$$

¹<https://github.com/shahanaibraimosu/mixed-membership-graph-clustering>

Then, the vector $\mathbf{m}_n = [m_{1,n}, \dots, m_{K,n}]^\top$ is referred to as the *membership vector* of data entity n , since it reflects the association of entity n with different clusters. All such vectors together constitute the *membership matrix* $\mathbf{M} = [\mathbf{m}_1, \dots, \mathbf{m}_N] \in \mathbb{R}^{K \times N}$.

In graph clustering, the entities are the nodes of the graph, and the relationship between the nodes are represented as the edges of the graph. In this work, we consider undirected graphs that are represented as symmetric adjacency matrices, i.e., $\mathbf{A} \in \{0, 1\}^{N \times N}$, where each entry $\mathbf{A}(i, j)$ encodes the pairwise relationship between nodes i and j in terms of binary values (i.e., $\mathbf{A}(i, j) \in \{0, 1\}$). Our goal is to learn the membership vector \mathbf{m}_n for each node from limited edge queries about the adjacency matrix \mathbf{A} (i.e., the number of edges queried is much smaller than total number of edges, i.e., $N(N - 1)/2$).

2.1 Motivating Examples

Our problem setting is motivated by a couple of important applications, namely, the crowdclustering problem and incomplete graph based overlapping community detection.

2.1.1 Example 1: Crowdclustering

Crowdclustering is a technique that clusters data samples with the assistance from crowdsourced annotators [7, 15, 16, 20, 22, 23]. In crowdclustering, the data entities are presented to the annotators in pairs. The annotators determine if the pair of entities are from the same category or not; i.e., the annotators apply a rule such that $\mathbf{A}(i, j) = 1$ if entities i, j ($i < j$) are believed to be from the same cluster, and $\mathbf{A}(i, j) = 0$ otherwise. Instead of asking the annotators to determine the exact membership of the n th data entity (i.e., the \mathbf{m}_n vector), the above mentioned rule only asks the annotators to output binary labels (i.e., if two entities are similar or not). This annotation paradigm is arguably more accurate than exact membership labeling, since it can work under much less expertise.

Crowdclustering amounts to learning \mathbf{m}_n from \mathbf{A} , which is a graph clustering problem. The challenge is that annotating the full adjacency graph means that $O(N^2)$ pairs have to be compared and labeled—a heavy workload if large data sets are considered. The works in [7, 15, 16, 20, 22, 23] randomly choose the data pairs to annotate—i.e., the methods use random edge queries. However, these methods can only handle the single membership case, and their nuclear norm-based convex optimization algorithms are computationally costly.

2.1.2 Example 2: Edge Sampling-Based Overlapping Community Detection

The mixed membership modeling in (1) and the learning problem of interest can also be applied to *overlapping community detection* (OCD) [24]—since the mixed membership setting implies that the communities have overlaps. Classic OCD algorithms work with statistical generative models, e.g., the *mixed membership stochastic blockmodel* (MMSB) [4, 25] and the *Bayesian nonnegative matrix factorization model* [26]. The mixed membership identifiability guarantees were established under full observation of \mathbf{A} in [25–28]. Mixed membership identification for OCD under sampled edges is of great interest for applications like field survey based community analysis [19] or community detection in link-removed/hidden networks (e.g., terrorist networks) [12]. In both cases, one may not be able to observe the entire \mathbf{A} due to reasons such as resource limitations and difficulty of edge acquisition. However, theoretical guarantees and provable algorithms for this problem have been elusive.

2.2 Prior Work

A theoretical challenge associated with our problem is as follows: Is it possible to learn the membership vector \mathbf{m}_n from the binary matrix \mathbf{A} ? This gives rise to a membership *identifiability* problem. If \mathbf{A} is fully observed, answering the identifiability question amounts to understanding theoretical guarantees for similarity graph-based membership learning techniques, e.g., MMSB identification and spectral clustering—which has been thoroughly studied in the machine learning community; see, e.g., [2, 25, 27, 28, 28]. However, when \mathbf{A} is only partially observed, the identifiability problem has not been fully understood.

To handle the graph clustering problem with partial observations, the work in [15, 16] models the generating process of \mathbf{A} using the SBM followed by a random edge query stage for data acquisition. The SBM can be summarized as follows. Assume that $\mathbf{B} \in \mathbb{R}^{K \times K}$ represents a cluster-cluster similarity matrix which is symmetric and $\mathbf{B}(p, q)$ represents the probability that cluster p is connected with cluster q . In addition, assume that the nodes are connected through their membership identities. Then, the probability that $\mathbf{A}(i, j) = 1$ is $\mathbf{P}(i, j) = \mathbf{m}_i^\top \mathbf{B} \mathbf{m}_j$, i.e., $\mathbf{A}(i, j) \sim \text{Bernoulli}(\mathbf{m}_i^\top \mathbf{B} \mathbf{m}_j)$ where $i < j$ —the adjacency matrix \mathbf{A} is sampled from Bernoulli distributions specified by the entries of the matrix $\mathbf{P} = \mathbf{M}^\top \mathbf{B} \mathbf{M}$. Note that under SBM, the membership vector \mathbf{m}_i is always a unit vector; i.e., only single membership and disjoint clusters are considered under SBM.

To recover \mathbf{M} from partially observed \mathbf{A} under SBM, the work in [15–17, 29] use the following convex program and its variants:

$$\underset{\mathbf{L} \in \{0,1\}^{N \times N}, \mathbf{S}}{\text{minimize}} \quad \|\mathbf{L}\|_* + \lambda \|\mathbf{S}\|_1 \tag{2a}$$

$$\text{subject to } \mathbf{L}(i, j) + \mathbf{S}(i, j) = \mathbf{A}(i, j), \quad \forall (i, j) \in \Omega. \tag{2b}$$

In the above, \mathbf{L} is used to model the low-rank component of \mathbf{A} , \mathbf{S} is a sparse error matrix, and Ω denotes the set of pairs (i, j) such that the corresponding $\mathbf{A}(i, j)$'s are observed. Notably, it was shown in [15–17] that if \mathbf{A} follows the SBM, then the above convex program (and its variants) recovers \mathbf{A} up to certain errors with provable guarantees using *random* edge queries. The results from [15–17] have opened many doors for edge query-based graph clustering, but several caveats exist. In particular, the recoverability is established based on single membership models, but the mixed membership case is of more interest. In addition, the optimization problem involves $O(N^2)$ variables (memory $\approx 3,000\text{GB}$ when $N = 10^6$), and thus is hardly scalable. Perhaps more critically, the provable guarantees in [15–17] rely on random edge query, which may not be easy to implement under some scenarios, as we discussed.

3 Proposed Approach

In this work, we relax the SBM assumption on $\mathbf{P} = \mathbf{M}^\top \mathbf{B} \mathbf{M}$ by allowing the nodes to have mixed membership. Hence, the constraints on \mathbf{M} becomes

$$\mathbf{1}^\top \mathbf{M} = \mathbf{1}^\top, \quad \mathbf{M} \geq \mathbf{0}; \tag{3}$$

i.e., \mathbf{m}_n resides in the probability simplex, instead of being the vertices of the simplex as in the SBM. Under the mixed membership assumption in (3), the following Bernoulli model, i.e.,

$$\begin{cases} \mathbf{A}(i, j) \sim \text{Bernoulli}(\mathbf{m}_i^\top \mathbf{B} \mathbf{m}_j), & i < j, \\ \mathbf{A}(i, j) = \mathbf{A}(j, i), & i > j, \\ \mathbf{A}(i, i) = 0, & i \in [N], \end{cases} \quad (4)$$

is adopted in our generative model for the complete adjacency matrix. Note that $\mathbf{m}_i^\top \mathbf{B} \mathbf{m}_j$ physically corresponds to the probability that nodes i and j admit an edge (i.e., $\Pr(\mathbf{A}(i, j) = 1) = \mathbf{m}_i^\top \mathbf{B} \mathbf{m}_j$), and thus this Bernoulli model makes intuitive sense. Overall, (3) and (4) present a model that is reminiscent of the MMSB model in OCD [4]

3.1 Systematic Edge Query

Our goal is to learn \mathbf{M} from controlled edge sampling strategies. To proceed, we first divide the nodes into L disjoint groups $\mathcal{S}_1, \mathcal{S}_2, \dots, \mathcal{S}_L$ such that $\mathcal{S}_1 \cup \dots \cup \mathcal{S}_L = [N]$. Let $\mathbf{A}_{\ell, m} \in \mathbb{R}^{|\mathcal{S}_\ell| \times |\mathcal{S}_m|}$ denote the adjacency matrix between groups of nodes indexed by \mathcal{S}_ℓ and \mathcal{S}_m . We propose an edge query principle as described in the following:

Edge Query Principle (EQP). Query the blocks of edges such that the sampled $\mathbf{A}_{\ell, m}$'s satisfy the following two conditions:

- For every $\ell \in [L]$, $K \leq |\mathcal{S}_\ell|$ holds.
- Let $m_r \in [L]$ and $\{\ell_r\}_{r=1}^L = [L]$. For every ℓ_r , there exists a pair of indices m_r and ℓ_{r+1} where $\ell_{r+1} \neq \ell_r$ such that the edges from the blocks \mathbf{A}_{ℓ_r, m_r} and $\mathbf{A}_{\ell_{r+1}, m_r}$ are queried.

Note that since \mathbf{A} is symmetric, when we select a block $\mathbf{A}_{\ell, m}$ to be queried, it also covers $\mathbf{A}_{m, \ell}$ since $\mathbf{A}_{m, \ell} = \mathbf{A}_{\ell, m}^\top$. A couple of remarks are in order:

Remark 1 *The proposed EQP covers a large variety of query ‘masks’—as shown in Fig. 1. Since the query pattern can be by design instead of random, this entails the flexibility to avoid querying edges that are known a priori hard to acquire, e.g., edges that may have been intentionally removed to conceal information or edges that correspond to interactions between groups that are hard to survey due to various reasons, e.g., long geographical distance.*

Remark 2 *Instead of sampling individual edges, we sample blocks of edges under the proposed EQP. As one will see, this simple block query pattern allows us to design a provable and lightweight algorithm for mixed membership learning. This block query strategy can be easily implemented when the query patterns are controlled by the network analysts. For example, in crowdclustering, one can dispatch blocks of sample pairs for similarity annotation. In community analysis, field surveys can be designed using EQP such that the blocks which are easier to be queried are selected.*

3.2 Connections to Matrix Completion

From a matrix completion viewpoint, our EQP is most closely related to those in [30, 31] that consider recoverable sampling patterns of matrix completion (MC). The work in [30] relates the

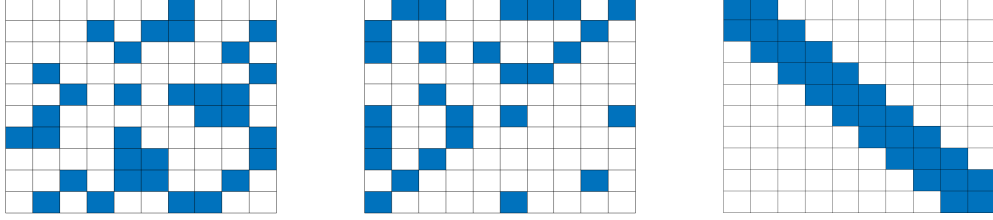


Figure 1: Some example patterns for \mathbf{A} following EQP with $N = 1000, K = 5$ and $L = 10$. The shaded blue region represents the blocks queried.

recoverability of a low-rank matrix to the structural properties of a bipartite graph by considering the rows and columns as nodes. It establishes the “finite” (not unique) completability of the matrix based on combinatorial conditions on the observed edges in its subgraphs. In a similar spirit, the work in [31] shows that the range space of a low-rank matrix can be uniquely identified under the existence of certain patterns formed by the sampled entries.

From an MC perspective, our block sampling pattern can be considered as special cases covered by those in [30, 31]—with important distinguishing features. First, the work in [30, 31] established recoverability under the sampling pattern, but had no tractable algorithms. Our EQP features a polynomial-time lightweight algorithm via exploiting the special block sampling pattern. Second, the recoverability results in [30, 31] only cover sampled continuous real-valued low-rank matrices without noise. Our approach can provably estimate the range space of binary matrices (or, highly noisy low-rank matrices) under reasonable conditions.

3.3 Algorithm Design

In this section, we propose an algorithm under the EQP. Specifically, under the considered model in (4), we develop an algorithm that consists of simple SVD operations to estimate $\text{range}(\mathbf{M}^\top)$ and a subsequent SSMF stage to ‘extract’ \mathbf{M} from the estimated range space.

3.3.1 Main Idea: A Toy Example

To shed some light on how our algorithm approximately identifies $\text{range}(\mathbf{M}^\top)$, let us consider the ideal case where $\mathbf{A}_{\ell,m} = \mathbf{P}_{\ell,m} = \mathbf{M}_\ell^\top \mathbf{B} \mathbf{M}_m$. We start by analyzing a toy example with $L = 3$ and $K \leq N/3$; see Fig. 2. We assume that the blocks $\mathbf{P}_{1,2} \in \mathbb{R}^{N/3 \times N/3}$, $\mathbf{P}_{2,2} \in \mathbb{R}^{N/3 \times N/3}$, and $\mathbf{P}_{3,1} \in \mathbb{R}^{N/3 \times N/3}$ are queried. Hence, by symmetry, the following blocks are known:

$$\mathbf{P}_{1,2} = \mathbf{M}_1^\top \mathbf{B} \mathbf{M}_2, \quad \mathbf{P}_{2,2} = \mathbf{M}_2^\top \mathbf{B} \mathbf{M}_2, \quad \mathbf{P}_{2,1} = \mathbf{M}_2^\top \mathbf{B} \mathbf{M}_1, \quad \mathbf{P}_{3,1} = \mathbf{M}_3^\top \mathbf{B} \mathbf{M}_1, \quad (5)$$

Define $\mathbf{C}_1 := [\mathbf{P}_{1,2}^\top, \mathbf{P}_{2,2}^\top]^\top$ and $\mathbf{C}_2 := [\mathbf{P}_{2,1}^\top, \mathbf{P}_{3,1}^\top]^\top$. The top- K SVD of \mathbf{C}_1 and \mathbf{C}_2 can be represented as follows:

$$\mathbf{C}_1 = [\mathbf{U}_1^\top, \mathbf{U}_2^\top]^\top \boldsymbol{\Sigma} \mathbf{V}_2^\top, \quad \mathbf{C}_2 = [\bar{\mathbf{U}}_2^\top, \bar{\mathbf{U}}_3^\top]^\top \bar{\boldsymbol{\Sigma}} \bar{\mathbf{V}}_1^\top. \quad (6)$$

Combining (5)-(6), and under the assumption that $\text{rank}(\mathbf{M}_\ell) = \text{rank}(\mathbf{B}) = K$ and $K \leq |\mathcal{S}_\ell|$, for all ℓ , one can express the bases of $\text{range}(\mathbf{M}_1^\top)$, $\text{range}(\mathbf{M}_2^\top)$ and $\text{range}(\mathbf{M}_3^\top)$ as $\mathbf{U}_1 = \mathbf{M}_1^\top \mathbf{G}$, $\mathbf{U}_2 = \mathbf{M}_2^\top \mathbf{G}$,

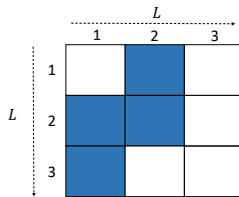


Figure 2: An illustrative case for subspace identifiability analysis.

$\bar{U}_3 = \mathbf{M}_3^\top \bar{\mathbf{G}}$, respectively, where $\mathbf{G} \in \mathbb{R}^{K \times K}$ and $\bar{\mathbf{G}} \in \mathbb{R}^{K \times K}$ are certain nonsingular matrices. Our hope is to “stitch” the bases above to have

$$\text{range}(\mathbf{U}) = \text{range}([\mathbf{U}_1^\top, \mathbf{U}_2^\top, \mathbf{U}_3^\top]^\top) = \text{range}([\mathbf{M}_1, \mathbf{M}_2, \mathbf{M}_3]^\top), \quad (7)$$

with \mathbf{U}_1 and \mathbf{U}_2 in (6) and a certain \mathbf{U}_3 . Note that \bar{U}_3 cannot be directly combined with \mathbf{U}_1 and \mathbf{U}_2 to attain the above, since $\mathbf{G} = \bar{\mathbf{G}}$ does not generally hold. To fix this, we define the following: $\mathbf{U}_3 := \bar{U}_3 \bar{U}_2^\dagger \mathbf{U}_2$. It is not hard to see that $\bar{U}_3 \bar{U}_2^\dagger \mathbf{U}_2 = \mathbf{M}_3^\top \bar{\mathbf{G}} \times (\mathbf{M}_2^\top \bar{\mathbf{G}})^\dagger \times \mathbf{M}_2^\top \mathbf{G} = \mathbf{M}_3^\top \mathbf{G}$, which leads to (7). The idea conveyed by this simple example can be recursively applied to cover a general L block case under the proposed EQP, and the range space estimation accuracy can be guaranteed even when \mathbf{A} is a noisy (binary) version of \mathbf{P} —which will be detailed in the next part. After $\mathbf{U}^\top = \mathbf{G}^\top \mathbf{M}$ is obtained, extracting \mathbf{M} from \mathbf{U}^\top is the so-called SSMF problem, which has been extensively studied; see a survey in [32].

3.3.2 Proposed Algorithm

In a similar spirit as alluded in the toy example, we propose Algorithm 1 (which is referred to as the *block edge query-based graph clustering* (BeQuec) algorithm). One can see that the BeQuec algorithm only consists of top- K SVD and least squares, which can be applied to very large graphs as long as K is of a moderate size. The SSMF stage (carried out by the *successive projection algorithm* (SPA)) is a Gram–Schmidt type algorithm that is also scalable (see Algorithm 2). Note that in Algorithm 1, \mathbf{U}_{ref1} and \mathbf{U}_{ref2} are temporary variables defined to pass the subspace estimated in the current iteration to the subsequent iteration. We further explain the two major stages of BeQuec, namely, the range space estimation stage and the membership extraction stage as follows.

Algorithm 1 Proposed Algorithm: BeQuec

Require: $L, K, \{\mathbf{A}_{\ell_r, m_r}\}_{r=1}^L, \{\mathbf{A}_{\ell_{r+1}, m_r}\}_{r=1}^{L-1}$ (where $\ell_r \neq \ell_{r+1}, \{\ell_r\}_{r=1}^L = [L], m_r \in [L], K \leq |\mathcal{S}_{\ell_r}|$)

- 1: $T \leftarrow \lfloor L/2 \rfloor$;
 - 2: $\mathbf{C}_T \leftarrow [\mathbf{A}_{\ell_T, m_T}^\top, \mathbf{A}_{\ell_{T+1}, m_T}^\top]^\top$;
 - 3: $[\mathbf{U}_{\ell_T}^\top, \mathbf{U}_{\ell_{T+1}}^\top]^\top \Sigma_T \mathbf{V}_{m_T}^\top \leftarrow \text{svd}_K(\mathbf{C}_T)$;
 - 4: $[\mathbf{U}_{\text{ref2}}^\top, \mathbf{U}_{\text{ref1}}^\top]^\top \leftarrow [\mathbf{U}_{\ell_T}^\top, \mathbf{U}_{\ell_{T+1}}^\top]^\top$;
 - 5: **for** $r = T + 1 : 1 : L - 1$ **do**
 - 6: $\mathbf{C}_r \leftarrow [\mathbf{A}_{\ell_r, m_r}^\top, \mathbf{A}_{\ell_{r+1}, m_r}^\top]^\top$;
 - 7: $[\bar{\mathbf{U}}_{\ell_r}^\top, \bar{\mathbf{U}}_{\ell_{r+1}}^\top]^\top \Sigma_r \mathbf{V}_{m_r}^\top \leftarrow \text{svd}_K(\mathbf{C}_r)$;
 - 8: $\mathbf{U}_{\ell_{r+1}} \leftarrow \bar{\mathbf{U}}_{\ell_{r+1}} \bar{\mathbf{U}}_{\ell_r}^\dagger \mathbf{U}_{\text{ref1}}$;
 - 9: $\mathbf{U}_{\text{ref1}} \leftarrow \mathbf{U}_{\ell_{r+1}}$;
 - 10: **end for**
 - 11: **for** $r = T : -1 : 2$ **do**
 - 12: $\mathbf{C}_r \leftarrow [\mathbf{A}_{\ell_{r-1}, m_{r-1}}^\top, \mathbf{A}_{\ell_r, m_{r-1}}^\top]^\top$;
 - 13: $[\bar{\mathbf{U}}_{\ell_{r-1}}^\top, \bar{\mathbf{U}}_{\ell_r}^\top]^\top \Sigma_r \mathbf{V}_{m_{r-1}}^\top \leftarrow \text{svd}_K(\mathbf{C}_r)$;
 - 14: $\mathbf{U}_{\ell_{r-1}} \leftarrow \bar{\mathbf{U}}_{\ell_{r-1}} \bar{\mathbf{U}}_{\ell_r}^\dagger \mathbf{U}_{\text{ref2}}$;
 - 15: $\mathbf{U}_{\text{ref2}} \leftarrow \mathbf{U}_{\ell_{r-1}}$;
 - 16: **end for**
 - 17: $\hat{\mathbf{U}} \leftarrow [\mathbf{U}_1^\top, \dots, \mathbf{U}_L^\top]^\top$;
 - 18: $\hat{\mathbf{G}}^\top \leftarrow \text{SPA}(\hat{\mathbf{U}}^\top, K)$ (see Algorithm 2);
 - 19: $\hat{\mathbf{M}} \leftarrow \arg \min_{\mathbf{M} \geq \mathbf{0}, \mathbf{1}^\top \mathbf{M} = \mathbf{1}^\top} \|\hat{\mathbf{U}}^\top - \hat{\mathbf{G}}^\top \mathbf{M}\|_F$ (or $\hat{\mathbf{M}} \leftarrow \hat{\mathbf{G}}^{-\top} \hat{\mathbf{U}}$);
 - 20: **return** $\hat{\mathbf{M}}$.
-

Algorithm 2 Successive Projection Algorithm (SPA) [33]

Require: \mathbf{X}, K

- 1: $\tilde{\mathbf{X}} \leftarrow \mathbf{X}$;
 - 2: **for** $k = 1 : K$ **do**
 - 3: $q_k \leftarrow \arg \max_{n \in [N]} \|\tilde{\mathbf{X}}(:, n)\|_2^2$;
 - 4: $\mathbf{u}_k \leftarrow \tilde{\mathbf{X}}(:, q_k)$;
 - 5: $\tilde{\mathbf{X}} \leftarrow \left(\mathbf{I}_K - \frac{\mathbf{u}_k \mathbf{u}_k^\top}{\|\mathbf{u}_k\|_2^2} \right) \tilde{\mathbf{X}}$;
 - 6: **end for**
 - 7: $\mathbf{W} \leftarrow \mathbf{X}(:, \{q_1, \dots, q_K\})$;
 - 8: **return** \mathbf{W} .
-

Sequential SVD for Range Space Estimation (Lines 1-17 in Algorithm 1) In a nutshell, BeQuec uses the idea from the toy example in an iterative fashion on the queried blocks \mathbf{A}_{ℓ_r, m_r} and $\mathbf{A}_{\ell_{r+1}, m_r}$ for $r = 1, \dots, L - 1$ —to estimate $\mathbf{U}^\top = \mathbf{G}^\top \mathbf{M}$, i.e., the range space of \mathbf{M}^\top . We start the iterations from $r = \lfloor L/2 \rfloor$ and perform the subspace stitching of the blocks in the ascending and descending orders, respectively—which helps reduce the subspace estimation error from the overall procedure, as will be seen in the analysis of Theorem 2.

SSMF for Membership Extraction (Lines 18-19 in Algorithm 1; Algorithm 2) If \mathbf{U} is perfectly estimated, the second stage estimates \mathbf{M} from the following SSMF model:

$$\mathbf{U}^\top = \mathbf{G}^\top \mathbf{M}, \quad \mathbf{M} \geq \mathbf{0}, \quad \mathbf{1}^\top \mathbf{M} = \mathbf{1}^\top, \quad (8)$$

where $\mathbf{G} \in \mathbb{R}^{K \times K}$ is nonsingular. The SSMF problem is the cornerstone of a number of core tasks in machine learning and signal processing, e.g., hyperspectral unmixing and topic modeling, which admits a plethora of algorithms for provably estimating \mathbf{M} under certain conditions [32]. To be precise, line 18 of Algorithm 1 invokes an SSMF algorithm, namely, SPA [33]. SPA is a lightweight algorithm which provably identifies \mathbf{M} from the model in (8) using K iterations and its per-iteration complexity is $O(NK^2)$ operations—under the assumption that some \mathbf{m}_n 's are close to single membership vectors (i.e., the existence of ‘pure/anchor nodes’ [25, 27, 28]). In general, the *anchor node assumption* is reasonable but not checkable. As one will see later (in Theorem 2), this assumption translates to that the number of nodes exceeds a certain threshold, if \mathbf{m}_n follows a reasonable generative model. This is reminiscent of a recent work in [34] that reveals the relation between the size of a nonnegative matrix and the so-called *separability* condition, as will be detailed in the proof of Theorem 2.

3.4 Performance Analysis

3.4.1 Complexity

Note that Algorithm 1 only consists of top- K SVD on small blocks that have a size of $2(N/L) \times (N/L)$ assuming $|\mathcal{S}_\ell| = N/L$ for all ℓ , which has a complexity of $O((N/L)K^2)$ flops—a similar complexity order of the SPA stage. In terms of memory, the process never needs to instantiate any $N \times N$ matrix that is used in the convex programming based methods [cf. (2)]. Instead, the variables involved are with the size of $N \times K$, thereby being economical in terms of memory (since the number of clusters K is often much smaller than N).

3.4.2 Accuracy

We first use the ideal case where $\mathbf{A}(i, j) = \mathbf{P}(i, j)$ to illustrate the key idea behind our proposed approach. Building on the understanding to the ideal noiseless case, the binary observation case, i.e., the model in (4), will be analyzed by treating it as a noisy version of the ideal case, with extensive care paid to the noise induced by the Bernoulli observation process. To be specific, we have the following subspace identification result:

Theorem 1 (*Ideal Case*) *Assume that $\mathbf{A}_{\ell, m} = \mathbf{P}_{\ell, m} = \mathbf{M}_\ell^\top \mathbf{B} \mathbf{M}_m \in \mathbb{R}^{|\mathcal{S}_\ell| \times |\mathcal{S}_m|}$ holds true for all $\ell, m \in [L]$ and $\text{rank}(\mathbf{M}_\ell) = \text{rank}(\mathbf{B}) = K$. Suppose that the $\mathbf{A}_{\ell, m}$'s are queried according to the proposed EQP. Then, the output $\hat{\mathbf{U}}$ by Algorithm 1 satisfies $\text{range}(\hat{\mathbf{U}}) = \text{range}(\mathbf{M}^\top)$.*

The proof of the theorem is relegated to Sec. A. The proof showcases how the range spaces of \mathbf{M}_ℓ^\top 's are ‘stitched’ together to recover $\text{range}(\mathbf{M}^\top)$, if $\mathbf{A}_{\ell, m} = \mathbf{P}_{\ell, m}$. In practice, however, the Bernoulli distribution parameters (i.e., the $\mathbf{P}_{\ell, m}$'s) are not observed. Instead, one observes $\mathbf{A}_{\ell, m}$'s with binary values, following the Bernoulli observation model in (4). The Bernoulli observation process can be understood as a noisy data acquisition process. To characterize the performance under this noisy case, we consider the following generative model:

Assumption 1 *The columns \mathbf{m}_n for all $n \in [N]$ are drawn from the probability simplex uniformly at random and $\text{rank}(\mathbf{M}_\ell) = \text{rank}(\mathbf{B}) = K$, for every ℓ . The matrix \mathbf{A} is generated following (3) and (4), and that $\mathbf{A}_{\ell, m}$'s are queried following the EQP, with $|\mathcal{S}_\ell| = N/L$ for every ℓ , where N/L is an integer.*

We also consider the following assumption which implies that the condition numbers of \mathbf{M}_ℓ 's are bounded:

Assumption 2 *There exists positive constants $\alpha_{\min}, \alpha_{\max}$ and γ such that for every $\ell \in [L]$, we have $\sigma_{\max}(\mathbf{M}_\ell) \leq \alpha_{\max}$, $\sigma_{\min}(\mathbf{M}_\ell) \geq \alpha_{\min}$, and $\kappa(\mathbf{M}_\ell) \leq \gamma := \frac{\alpha_{\max}}{\alpha_{\min}}$.*

In addition, we adopt the following definition of node degree that is widely used in network analysis [35]:

Definition 1 *The degree of node i is the number of “similar nodes” it has in the adjacency graph; i.e., $\text{degree}(i) = \sum_{j=1}^N \mathbf{A}(i, j)$, where $\mathbf{A} \in \{0, 1\}^{N \times N}$.*

Using Assumptions 1-2 and the above definition, we show the following theorem:

Theorem 2 (Binary Observation Case) *Let $\rho := \max_{i,j} \mathbf{P}(i, j)$ be the maximal entry of \mathbf{P} . Suppose that $\rho = \Omega(L \log(N/L)/N)$ and $L = O(\rho N/d)$ where d is the maximal degree of all the nodes. Also assume that $N = \Omega\left(\max\left(L^2, \frac{\varepsilon^{-K}}{K} \log\left(\frac{NK}{L^2}\right), \frac{(K\gamma^2)^L \rho \kappa^2(\mathbf{B})}{\sigma_{\min}^2(\mathbf{B})}\right)\right)$ for a certain constant $0 \leq \varepsilon = O\left(\frac{1}{K\gamma^3}\right)$. Then, the output $\widehat{\mathbf{U}}$ and $\widehat{\mathbf{M}}$ by Algorithm 1 satisfies the following with probability of at least $1 - O(L^2/N)$:*

$$\|\widehat{\mathbf{U}} - \mathbf{U}\mathbf{O}\|_{\text{F}} = \zeta = O\left(\frac{(K\gamma^2)^{L/2} \kappa(\mathbf{B}) \sqrt{\rho}}{\sigma_{\min}(\mathbf{B}) \sqrt{N/L}}\right), \quad (9)$$

$$\min_{\mathbf{\Pi}} \|\widehat{\mathbf{M}} - \mathbf{\Pi}\mathbf{M}\|_{\text{F}} = O\left(K^2 \sigma_{\max}(\mathbf{M}) \gamma^3 \max(\varepsilon, \zeta)\right), \quad (10)$$

where \mathbf{U} is an orthogonal basis of $\text{range}(\mathbf{M}^\top)$, $\mathbf{O} \in \mathbb{R}^{K \times K}$ is an orthogonal matrix and $\mathbf{\Pi} \in \mathbb{R}^{K \times K}$ is a permutation matrix.

The proof can be found in Sec. B. From Theorem 2, one can see that if N is large enough, the BeQuec algorithm outputs a provably accurate estimate for the membership matrix \mathbf{M} under the proposed EQP. Theorem 2 has some important practical implications as well. First, the number of blocks in the query pattern design plays a critical role. On one hand, L cannot be too large, since L being too large may lead to the EQP condition $K \leq |\mathcal{S}_\ell| = N/L$ being violated. In addition, a larger L makes the error bound looser, since the factor $(K\gamma^2)^{L/2}$ increases quickly with L . On the other hand, a larger L means fewer queries need to be made, which means a better sample complexity of the procedure. Hence, the theorem reveals an important trade-off that is of interest to query designers.

3.4.3 More Discussion

Given the underlying structure of $\mathbf{A}_{\ell,k}$, a natural question is as follows: Instead of first estimating $\text{range}(\mathbf{M}^\top)$ and then estimating \mathbf{M} , why not estimate \mathbf{M}_m (or \mathbf{M}_ℓ) from $\mathbf{A}_{\ell,m}$ (using SSMF algorithms on $\mathbf{A}_{\ell,m} \approx \mathbf{M}_\ell^\top \mathbf{B} \mathbf{M}_m = \mathbf{G}_\ell^\top \mathbf{M}_m$) and then stitch them together to recover \mathbf{M} ? This is not infeasible—but is prone to failure due to various reasons. To be specific, to successfully extract the membership information from $\widehat{\mathbf{U}}^\top$ (resp. $\mathbf{A}_{\ell,m}$) using SPA, \mathbf{M} (resp. \mathbf{M}_m) needs to satisfy the *anchor node assumption* [27] (or, the *separability* condition in the context of SSMF [32, 33]). Geometrically, it means that some of the columns of \mathbf{M} (resp. \mathbf{M}_m) ‘touch’ all the vertices of

the probability simplex. If the columns of \mathbf{M} is drawn from the probability simplex uniformly at random (or following any joint continuous distribution), then a membership matrix that has more columns enjoys a much better chance to attain this condition [34]. Hence, working with $\widehat{\mathbf{U}}^\top \approx \mathbf{G}^\top \mathbf{M}$ to extract $\mathbf{M} \in \mathbb{R}^{K \times N}$ is preferred over working with $\mathbf{A}_{\ell,m} \approx \mathbf{G}_\ell^\top \mathbf{M}_m$ to extract $\mathbf{M}_m \in \mathbb{R}^{K \times (N/L)}$, since the former has a membership matrix that has more number of columns.

To be more precise, in order to make the complete membership matrix $\mathbf{M} \in \mathbb{R}^{K \times N}$ satisfy the anchor node assumption up to ε -violation with probability greater than $1 - \mu$, $N = \Omega\left(\frac{\varepsilon^{-2K}}{K} \log(K/\mu)\right)$ suffices under Assumption 1 ([34, Theorem 2]; also see Sec. B.2 in appendix for more details). On the other hand, for every \mathbf{M}_ℓ individually satisfying the anchor node assumption, one would need $N = \Omega\left(\frac{L^{K+1}\varepsilon^{-2K}}{K} \log(K/\mu)\right)$ to have the same guarantee—and the L^{K+1} factor could make a big difference. In addition, applying SSMF onto every $\mathbf{A}_{\ell,m}$ may make the procedure fairly ‘fragile’—if the SSMF fails to extract \mathbf{M}_ℓ from one block, then the entire procedure fails. Indeed, our experiments also show that this idea is not as competitive, as one will see in Sec. 4

4 Experiments

4.1 Baselines

For both synthetic and real data experiments, we compare our algorithm with a number of state-of-the-art mixed membership learning algorithms, namely, *geometric intuition-based nonnegative matrix factorization* (GeoNMF) [28], *community detection via minimum volume simplex identification* (CD-MVSI) [25], and *community detection via Bayesian nonnegative matrix factorization* (CD-BNMF) [26]. These baselines are applied onto the queried blocks (e.g., $\mathbf{A}_{\ell,m}$) to estimate \mathbf{M}_ℓ and \mathbf{M}_m , as discussed in Sec. 3.4.3. The estimated \mathbf{M}_ℓ ’s are aligned (by a nontrivial aligning procedure) to unify the row permutation ambiguity. This step is necessary since the estimated \mathbf{M}_ℓ ’s from different blocks are subject to different row permutation ambiguities; see details in Sec. K of the supplemental material. We have two different sets of real data experiments, i.e., crowdclustering of dog breed image data and community detection in co-author networks. For real data experiments, we additionally apply two versions of the spectral clustering algorithm, namely, the unnormalized and normalized spectral clustering algorithms—denoted as SC (unnorm.) and SC (norm.), respectively [36]. We also use *k-means* and a convex optimization-based graph clustering algorithm with edge queries (denoted as Convex-Opt) [15] as benchmarks. We follow the setup in [15] and apply *k-means* directly on the adjacency graphs [denoted as *k-means* (graph)]. Note that in the crowdclustering experiment in Sec. 4.3 (also see Sec. 2.1 for the problem definition), we also use *k-means* on the original image samples [denoted as *k-means* (data)], since the raw data samples are available in this particular problem. The *k-means* (data) method serves as a basic benchmark where no annotator input is used. The source code and the real data used in our experiments are made publicly available (see Sec. 1.2).

4.2 Synthetic Data

We consider N nodes (where $N \in [1 \times 10^4, 8 \times 10^4]$) and $K = 5$ clusters. The membership vectors \mathbf{m}_n are drawn from the Dirichlet distribution with parameters being $(1/K)\mathbf{1}$, where $\mathbf{1}$ is a K -dimensional all-one vector. The cluster-cluster interaction matrix $\mathbf{B} \in \mathbb{R}^{K \times K}$ is generated as follows: First, a symmetric matrix is generated, whose upper triangular entries are sampled

Table 1: The subspace distance between $\text{range}(\hat{\mathbf{U}})$ and $\text{range}(\mathbf{M}^\top)$ and MSE of \mathbf{M} for ideal and binary observation cases; $K = 5$, $L = 10$ (percentage of queried edges = 27.92%).

Graph Size	Ideal Case	Binary Observation Case				
	BeQuec (proposed)	BeQuec (proposed)	GeoNMF	CD-MVSI	CD-BNMF	
N	Dist	Dist	MSE	MSE	MSE	MSE
1×10^4	7.34×10^{-13}	0.342	0.0475	0.0554	0.0839	0.0559
2×10^4	2.80×10^{-13}	0.209	0.0198	0.0386	0.0943	0.0602
4×10^4	1.22×10^{-13}	0.194	0.0123	0.0341	0.0955	0.0649
8×10^4	1.12×10^{-13}	0.101	0.0066	0.0261	0.0924	0.0700

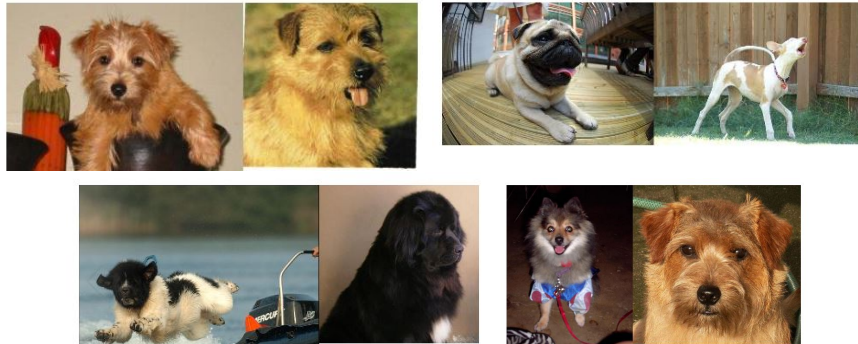


Figure 3: Some examples of the pairs presented to the AMT annotators in the crowdclustering experiment. The image pairs have true similarity labels 1,0,0,1, respectively, in clockwise order. The annotators marked 1,0,1,0, respectively.

uniformly at random from the range $[0, 1]$. Second, an identity matrix \mathbf{I}_K is added to the generated matrix. Finally, all the resultant entries are down-scaled by the same scalar to make sure that they lie in between 0 and 1. This way, \mathbf{B} is diagonal dominant, since in-cluster interactions is more likely to happen.

We first test the identifiability claims under the ideal case (i.e., $\mathbf{A} = \mathbf{P}$). The blocks of the adjacency matrix with the leftmost query pattern in Fig. 1 is used. We fix the number of groups to be $L = 10$. Table 1 shows the subspace estimation accuracy of our method. The performance is measured using the subspace distance (denoted as ‘Dist’) between $\text{range}(\hat{\mathbf{U}})$ and the ground-truth $\text{range}(\mathbf{M}^\top)$ (see definition of subspace distance in [37]) under different N ’s. The results are averaged from 20 random trials. One can see that the proposed method estimates the subspace of the membership matrix \mathbf{M} very accurately, which verifies our subspace identifiability analysis in Theorem 1.

Next, we consider the rightmost pattern in Fig 1 to evaluate the proposed algorithm and the baselines in the binary observation case (i.e., following the Bernoulli model in (4)). The results can also be found in Table 1, which shows the subspace distance and *mean squared error* (MSE) of the estimated \mathbf{M} (see definition in [38]) averaged over 20 random trials. One can see that, the subspace estimation error of the proposed algorithm gets smaller as N grows, as Theorem 2 indicates. In all the cases, the proposed method outperforms the baseline methods in terms of MSE of \mathbf{M} . Recall that the baselines estimate \mathbf{M}_ℓ ’s from individual blocks and our method estimates \mathbf{M} from the recovered $\hat{\mathbf{U}}$. This echos our discussions in Sec. 3.4.3—i.e., the \mathbf{M} identification part works better when one has a “fatter” membership matrix.

Table 2: Graph clustering performance on the dog breed dataset with AMT similarity annotations. $N = 900, K = 5, L = 15$. Annotation proportion = 19.02%.

Algorithms	ACC (%)	NMI	Time (s)
BeQuec (proposed)	99.22	0.972	0.21
GeoNMF	96.88	0.929	2.80
CD-MVSI	38.02	0.199	1.30
CD-BNMF	81.89	0.683	0.28
SC (unnorm.)	23.58	0.040	0.38
SC (norm.)	86.89	0.829	0.39
k -means (graph)	66.44	0.502	0.11
k -means (data)	23.00	0.005	520.97
Convex-Opt	30.58	0.109	53.78

Table 3: Graph clustering performance on the dog breed dataset for different annotation error rates. $N = 900, K = 5, L = 15$. Annotation proportion = 19.02%.

Algorithms	annotation error=15%		annotation error=20%	
	ACC(%)	NMI	ACC(%)	NMI
BeQuec (proposed)	95.83	0.941	87.20	0.740
GeoNMF	85.33	0.688	79.83	0.629
CD-MVSI	42.28	0.194	38.57	0.165
CD-BNMF	67.64	0.609	66.89	0.574
SC (unnorm.)	24.52	0.046	24.63	0.036
SC (norm.)	69.21	0.573	69.10	0.558
k -means (graph)	60.27	0.465	59.42	0.489
Convex-Opt	25.74	0.021	23.56	0.008

4.3 Crowdclustering for AMT Data

We consider the task of clustering a set of images of dogs into different breeds with the assistance of self-registered annotators from a crowdourcing platform, i.e., the AMT platform.

AMT Data We upload $N = 900$ images of $K = 5$ different breeds of dogs from the Stanford Dogs Dataset [39]. The chosen breeds are Pug (180 images), Ibizan Hound (180 images), Pomeranian (180 images), Norfolk Terrier (172 images) and Newfoundland (188 images). We followed the setup in Sec. 2.1 to design the experiment. Specifically, we showed each annotator a pair of dog images and ask a simple question (query): “Do this pair of dogs belong to the same category?”. If the annotator marks “Yes”, then we fill the corresponding entry of \mathbf{A} with “1”, and otherwise “0”. In this case, if one hopes to fill all the entries of \mathbf{A} , there are approximately 4×10^5 distinct pairs of images to be queried, which is costly. We selected image pairs following the block-diagonal pattern (i.e., the rightmost pattern in Fig. 1) by fixing $L = 15$. As a result, only 19.02% of the pairs (76,950) were queried². Fig. 3 shows some pairs of images queried in this experiment. We obtained the responses from 642 AMT annotators. Each annotator answered (non-overlapping) 120 queries on average. The error rate of the answers given by the annotators was 9.90%.

²As a result, \$81.60 was paid for our annotation task to AMT, but annotating all the pairs of images for this experiment would have cost \$429.02.

Table 4: Averaged SRC and runtime in seconds. $L = 10$ (percentage of queried edges = 27.92%).

Datasets (N, K)	BeQuec (proposed)		GeoNMF		CD-MVSI		CD-BNMF	
	SRC	Time(s.)	SRC	Time(s.)	SRC	Time(s.)	SRC	Time(s.)
DBLP ₋₁ (15075, 13)	0.177	0.47	0.075	15.87	0.074	0.95	0.058	5.61
DBLP ₋₂ (18106, 16)	0.166	0.38	0.089	11.13	0.055	0.76	0.070	8.20
DBLP ₋₃ (18646, 16)	0.166	0.46	0.076	17.18	0.064	0.98	0.060	8.50
DBLP ₋₄ (18195, 16)	0.191	0.48	0.098	15.76	0.070	0.95	0.079	8.50
DBLP ₋₅ (14982, 15)	0.195	0.41	0.084	15.65	0.073	0.88	0.074	5.85
MAG1 (37680, 3)	0.125	0.26	0.122	1.79	0.089	0.59	0.069	37.29
MAG2 (19457, 3)	0.441	0.23	0.240	4.66	0.249	0.53	0.122	9.92

Metric To quantify the performance, we use standard metrics for evaluating the clustering algorithms. Specifically, since each image is only labeled with a single cluster label, we round the learned membership vectors to the closest unit vectors. This way, standard metrics, i.e., *clustering accuracy* (ACC) and *normalized mutual information* (NMI) can be used for performance characterization (see definitions of ACC and NMI in [40]). ACC ranges from 0% to 100% where 100% means perfect clustering. NMI takes values in between 0 and 1 with 1 being the best performance.

Results Table 2 summarizes the results output by the algorithms under test. One can see that the proposed BeQuec method exhibits the highest ACC and NMI. In particular, BeQuec largely outperforms directly applying clustering methods to the data samples without annotators’ assistance [cf. *k-means* (data)]. Note that *k-means* (data) sees all the data and their features (pixels in this case). It does not work well perhaps because the dogs across some breeds are naturally confusing. However, with annotating less than 20% of the data pairs’ similarity (without pointing out the exact breeds), the clustering error approaches zero. This experiment may have articulated the value of this simple annotation strategy.

In Table 2, one can also see that GeoNMF and SC (norm.) work reasonably well, but less competitive compared to the proposed method. The proposed method also has a good runtime performance. Notably, BeQuec is almost 200 times faster than Convex-Opt and more than 10 times faster than GeoNMF.

In order to better understand the impact of annotation errors on crowdclustering, we also manually ‘inject’ some errors to the annotations. Specifically, we randomly flip a certain percentage of the correct annotations given by the AMT annotators, and observe how this affects the performance of the algorithms.

Table 3 presents the clustering performance obtained from two different error rates. The results are averaged over 20 trials, where in each trial the flipped annotations are randomly chosen. One can observe that the proposed BeQuec method still offers the most competitive clustering performance. When the annotation error rate increases from 9.9% (Table 2) to 15% and 20%, the performance degradation of BeQuec is much less obvious compared to the baselines. In particular, one can see that NMI of BeQuec decreases from 0.972 to 0.941 when the annotation error rate is changed from 9.9% to 15%. However, GeoNMF’s NMI changes from 0.929 to 0.688, which is a much more drastic drop. This shows BeQuec’s robustness to annotation errors.

Table 5: Clustering accuracy (%) of MAG2 under various L (percentage of queried edges (%)). $N = 19457$, $K = 3$.

Alorithms	$L = 10$ (27.92%)	$L = 25$ (11.58%)	$L = 50$ (5.82%)	$L = 75$ (3.86%)	$L = 100$ (2.87%)
BeQuec (proposed)	78.70	77.19	67.81	61.85	56.98
GeoNMF	58.16	57.87	56.88	52.68	52.33
CD-MVSI	53.45	21.82	14.57	13.53	11.71
CD-BNMF	51.19	49.35	49.37	48.99	48.97
SC (unnorm.)	49.95	52.81	55.48	55.50	55.07
SC (norm.)	64.80	67.29	59.80	52.70	55.90
k -means	50.28	51.56	53.46	54.25	54.27

4.4 Co-author Network Community Detection

We test the edge query-based graph clustering algorithms using the co-authorship network data from MAG [41] and DBLP [42]. In all the datasets, node-node connection (co-authorship) is represented by a binary value (“1” means that the two nodes have co-authored at least one paper and “0” means otherwise). For our experiments, we use the version of these networks published by the authors of [28]. Each network is provided with ground-truth mixed membership of the nodes. In these networks, nodes represent the authors of the research papers from different fields of study. Some nodes exhibit multiple memberships, since some authors publish in different fields.

MAG Data In our experiment, we use a subset of nodes that have a degree of at least 5. Consequently, two co-author networks, namely, MAG1 and MAG2, have 37,680 and 19,457 authors, respectively. In MAG1 and MAG2, all the authors are from 3 different fields of study, i.e., $K = 3$.

DBLP Data The 5 DBLP datasets (denoted as DBLP1, ..., DBLP5) used in [28] have 6176, 3145, 2605, 3056, and 6269 nodes, respectively. In addition, the number of clusters present in the DBLP datasets are 6, 3, 3, 3, and 4, respectively. To make the clustering problem more challenging, we combine the smaller original DBLP networks into larger-size networks following the setting in [25]. We use the notation DBLP $_{-i}$ to denote the network where all the 5 DBLP networks except the i -th one are combined. This way, different DBLP $_{-i}$ ’s can be produced for testing the algorithms. In addition, each DBLP $_{-i}$, for $i = 1, \dots, 5$, contains 13-16 clusters, presenting more challenging scenarios.

Metric The methods are evaluated using the averaged *Spearman’s rank correlation coefficient* (SRC), which is often used in the mixed membership learning literature (e.g., [25,28]). The averaged SRC takes values between -1 and 1 . SRC has a higher value if the ranking of the entries in two vectors are more similar—which is desired. We let all the algorithms to access only part of the network under the block-diagonal query pattern in Fig. 1. We randomize the node order in each of the 20 trials and present the averaged performance.

Results We first test the mixed membership learning performance by setting $L = 10$ for all the MAG and DBLP datasets under test. The percentage of edges queried in this setting is 27.92%. From Table 4, one can see that the proposed BeQuec algorithm consistently outperforms

the baselines in all the graphs under test. In addition, **BeQuec**'s runtime performance is also the most competitive.

Table 5 uses MAG2 dataset to show the performance of **BeQuec** under various L 's. We also apply the clustering algorithms used in crowdclustering to benchmark **BeQuec**'s performance. The ACC metric is used in this table since the clustering algorithms do not output mixed membership. One can see that the performance of all algorithms decreases along with L 's increase—which is consistent with our analysis in Theorem 2. For each L used, the corresponding queried percentage of edges is listed in the first row. Notably, when $L = 50$, i.e, only 5.82% of \mathbf{A} is observed, the proposed method still outputs a reasonable clustering accuracy. This demonstrates a promising balance between the query sample complexity and the graph clustering accuracy.

5 Conclusion

In this work, we proposed a graph query scheme that enables provable graph clustering with partially observed edges. Unlike previous works relying on random graph edge query and computationally heavy convex programming, our method features a lightweight algorithm and works with systematic edge query patterns that are arguably more realistic in some applications. Our method also learns mixed membership of nodes from overlapping clusters, which improves upon existing provable graph query-based methods that work with single membership and disjoint clusters. We tested the proposed **BeQuec** algorithm on two real-world network data analytics problems, namely, crowdclustering and network community detection. **BeQuec** offers promising results in both experiments. Future work includes reducing the query sample complexity, e.g., by allowing $N/L < K$, and developing algorithms that may estimate the number of clusters and the membership simultaneously.

References

- [1] S. E. Schaeffer, “Graph clustering,” *Computer Science Review*, vol. 1, no. 1, pp. 27–64, 2007.
- [2] A. Y. Ng, M. I. Jordan, and Y. Weiss, “On spectral clustering: Analysis and an algorithm,” *Advances in Neural Information Processing Systems*, vol. 14, pp. 849–856, 2002.
- [3] S. White and P. Smyth, “A spectral clustering approach to finding communities in graphs,” *Proceedings of SIAM International Conference on Data Mining*, pp. 274–285, 2005.
- [4] E. M. Airoldi, D. M. Blei, S. E. Fienberg, and E. P. Xing, “Mixed membership stochastic blockmodels,” *Advances in Neural Information Processing Systems*, vol. 21, pp. 33–40, 2009.
- [5] D. Kuang, C. Ding, and H. Park, “Symmetric nonnegative matrix factorization for graph clustering,” *Proceedings of SIAM International Conference on Data Mining*, pp. 106–117, 2012.
- [6] S. Van Dongen, “Graph clustering via a discrete uncoupling process,” *SIAM Journal on Matrix Analysis and Applications*, vol. 30, no. 1, pp. 121–141, 2008.
- [7] A. Saade, M. Lelarge, F. Krzakala, and L. Zdeborová, “Clustering from sparse pairwise measurements,” *IEEE International Symposium on Information Theory*, pp. 780–784, 2016.

- [8] Y. Zhang, E. Levina, and J. Zhu, “Detecting overlapping communities in networks using spectral methods,” *SIAM Journal on Mathematics of Data Science*, vol. 2, no. 2, pp. 265–283, 2020.
- [9] M. T. Schaub, S. Segarra, and J. N. Tsitsiklis, “Blind identification of stochastic block models from dynamical observations,” *SIAM Journal on Mathematics of Data Science*, vol. 2, no. 2, pp. 335–367, 2020.
- [10] J. Leskovec and C. Faloutsos, “Sampling from large graphs,” *Proceedings of ACM International Conference on Knowledge Discovery and Data Mining*, p. 631–636, 2006.
- [11] P. Hu and W. C. Lau, “A survey and taxonomy of graph sampling,” *Computing Research Repository*, 2013.
- [12] M. J. Salganik and D. D. Heckathorn, “Sampling and estimation in hidden populations using respondent-driven sampling,” *Sociological Methodology*, vol. 34, no. 1, pp. 193–240, 2004.
- [13] M. Malekinejad, L. Johnston, C. Kendall, L. R. Kerr, M. Rifkin, and G. Rutherford, “Using respondent-driven sampling methodology for hiv biological and behavioral surveillance in international settings: A systematic review,” *AIDS and Behavior*, vol. 12, pp. 5–30, 07 2008.
- [14] K. A. Gill and M. O’Neal, “Survey of Soybean Insect Pollinators: Community Identification and Sampling Method Analysis,” *Environmental Entomology*, vol. 44, no. 3, pp. 488–498, 02 2015.
- [15] R. Korlakai Vinayak, S. Oymak, and B. Hassibi, “Graph clustering with missing data: Convex algorithms and analysis,” *Advances in Neural Information Processing Systems*, vol. 27, pp. 2996–3004, 2014.
- [16] R. Korlakai Vinayak and B. Hassibi, “Crowdsourced clustering: Querying edges vs triangles,” *Advances in Neural Information Processing Systems*, vol. 29, pp. 1316–1324, 2016.
- [17] Y. Chen, A. Jalali, S. Sanghavi, and H. Xu, “Clustering partially observed graphs via convex optimization,” *Journal of Machine Learning Research*, vol. 15, no. 1, pp. 2213–2238, 2014.
- [18] K. Rohe, S. Chatterjee, B. Yu *et al.*, “Spectral clustering and the high-dimensional stochastic blockmodel,” *Annals of Statistics*, vol. 39, no. 4, pp. 1878–1915, 2011.
- [19] C. Särndal, B. Swensson, and J. Wretman, *Model Assisted Survey Sampling*, ser. Springer Series in Statistics. Springer-Verlag, 2003.
- [20] J. Yi, R. Jin, S. Jain, T. Yang, and A. K. Jain, “Semi-crowdsourced clustering: Generalizing crowd labeling by robust distance metric learning,” *Advances in Neural Information Processing Systems*, vol. 25, pp. 1772–1780, 2012.
- [21] S. Ibrahim and X. Fu, “Learning mixed membership from adjacency graph via systematic edge query: Identifiability and algorithm,” submitted to *International Conference on Acoustics, Speech, and Signal Processing*, Aug 2021.
- [22] R. G. Gomes, P. Welinder, A. Krause, and P. Perona, “Crowdclustering,” *Advances in Neural Information Processing Systems*, vol. 24, pp. 558–566, 2011.

- [23] J. Yi, R. Jin, A. Jain, and S. Jain, “Crowdclustering with sparse pairwise labels: A matrix completion approach,” in *AAAI Workshop on Human Computation*, 2012.
- [24] J. Xie, S. Kelley, and B. K. Szymanski, “Overlapping community detection in networks: The state-of-the-art and comparative study,” *ACM Computing Surveys*, vol. 45, no. 4, Aug. 2013.
- [25] K. Huang and X. Fu, “Detecting overlapping and correlated communities without pure nodes: Identifiability and algorithm,” *Proceedings of International Conference on Machine Learning*, vol. 97, pp. 2859–2868, 2019.
- [26] I. Psorakis, S. Roberts, M. Ebden, and B. Sheldon, “Overlapping community detection using bayesian non-negative matrix factorization,” *Physical Review E*, vol. 83, p. 066114, 06 2011.
- [27] M. Panov, K. Slavnov, and R. Ushakov, “Consistent estimation of mixed memberships with successive projections,” *Complex Networks*, p. 53–64, 2017.
- [28] X. Mao, P. Sarkar, and D. Chakrabarti, “On mixed memberships and symmetric nonnegative matrix factorizations,” in *International Conference on Machine Learning*, 2017, pp. 2324–2333.
- [29] S. Oymak and B. Hassibi, “Finding dense clusters via ”low rank + sparse” decomposition,” *Computing Research Repository*, 04 2011.
- [30] F. J. Király, L. Theran, and R. Tomioka, “The algebraic combinatorial approach for low-rank matrix completion,” *Journal of Machine Learning Research*, vol. 16, no. 41, pp. 1391–1436, 2015.
- [31] D. L. Pimentel-Alarcón, N. Boston, and R. D. Nowak, “A characterization of deterministic sampling patterns for low-rank matrix completion,” *IEEE J. Sel. Topics Signal Process.*, vol. 10, no. 4, pp. 623–636, 2016.
- [32] X. Fu, K. Huang, N. D. Sidiropoulos, and W.-K. Ma, “Nonnegative matrix factorization for signal and data analytics: Identifiability, algorithms, and applications,” *IEEE Signal Process. Mag.*, vol. 36, no. 2, pp. 59–80, 2019.
- [33] N. Gillis and S. Vavasis, “Fast and robust recursive algorithms for separable nonnegative matrix factorization,” *IEEE Trans. Pattern Anal. Mach. Intell.*, vol. 36, no. 4, pp. 698–714, April 2014.
- [34] S. Ibrahim, X. Fu, N. Kargas, and K. Huang, “Crowdsourcing via pairwise co-occurrences: Identifiability and algorithms,” *Advances in Neural Information Processing Systems*, vol. 32, pp. 7847–7857, 2019.
- [35] U. Luxburg, “A tutorial on spectral clustering,” *Statistics and Computing*, vol. 17, no. 4, p. 395–416, Dec. 2007.
- [36] Jianbo Shi and J. Malik, “Normalized cuts and image segmentation,” *IEEE Trans. Pattern Anal. Mach. Intell.*, vol. 22, no. 8, pp. 888–905, 2000.
- [37] G. H. Golub and C. F. Van Loan, *Matrix computations*. JHU Press, 2012, vol. 3.

- [38] K. Huang, X. Fu, and N. D. Sidiropoulos, “Anchor-free correlated topic modeling: Identifiability and algorithm,” *Advances in Neural Information Processing Systems*, vol. 29, pp. 1786–1794, 2016.
- [39] A. Khosla, N. Jayadevaprakash, B. Yao, and L. Fei-Fei, “Novel dataset for fine-grained image categorization,” in *First Workshop on Fine-Grained Visual Categorization, IEEE Conference on Computer Vision and Pattern Recognition*, Colorado Springs, CO, June 2011.
- [40] C. Lu, J. Tang, M. Lin, L. Lin, S. Yan, and Z. Lin, “Correntropy induced l2 graph for robust subspace clustering,” *IEEE International Conference on Computer Vision*, pp. 1801–1808, 2013.
- [41] A. Sinha, Z. Shen, Y. Song, H. Ma, D. Eide, B. Hsu, and K. Wang, “An overview of microsoft academic service (mas) and applications,” *Proceedings of International Conference on World Wide Web*, p. 243–246, 2015.
- [42] M. Ley, “The DBLP computer science bibliography: Evolution, research issues, perspectives,” *Proceedings of International Symposium on String Processing and Information Retrieval*, pp. 1–10, 2002.
- [43] Y. Yu, T. Wang, and R. J. Samworth, “A useful variant of the Davis–Kahan theorem for statisticians,” *Biometrika*, vol. 102, no. 2, pp. 315–323, 04 2014.
- [44] J. Lei and A. Rinaldo, “Consistency of spectral clustering in stochastic block models,” *Annals of Statistics*, vol. 43, no. 1, pp. 215–237, 02 2015.
- [45] P. Wedin, “Perturbation theory for pseudo-inverses,” *BIT Numerical Mathematics*, vol. 13, pp. 217–232, 1973.
- [46] R. A. Horn and C. R. Johnson, *Matrix Analysis*, 2nd ed. USA: Cambridge University Press, 2012.
- [47] R. Jonker and T. Volgenant, “Improving the hungarian assignment algorithm,” *Operations Research Letters*, vol. 5, no. 4, pp. 171–175, 1986.

A Proof of Theorem 1

Algorithm 1 aims to output \widehat{U} such that $\text{range}(\widehat{U}) = \text{range}([M_1, \dots, M_L]^\top)$. It implies that $\widehat{U} = [U_1^\top, \dots, U_L^\top]^\top = [M_1, M_2, \dots, M_L]^\top G = M^\top G$, for a certain nonsingular $G \in \mathbb{R}^{K \times K}$. To show this, we start by considering the below four blocks for any $r \in [L - 2]$:

$$P_{\ell_r, m_r} = M_{\ell_r}^\top B M_{m_r}, \quad P_{\ell_{r+1}, m_r} = M_{\ell_{r+1}}^\top B M_{m_r}, \quad (11a)$$

$$P_{\ell_{r+1}, m_{r+1}} = M_{\ell_{r+1}}^\top B M_{m_{r+1}}, \quad P_{\ell_{r+2}, m_{r+1}} = M_{\ell_{r+2}}^\top B M_{m_{r+1}}. \quad (11b)$$

Algorithm 1 defines the following matrices in r th and $(r + 1)$ th iterations, respectively (recall that we have assumed $A_{\ell, m} = P_{\ell, m} = M_\ell^\top B M_m$ for any $\ell, m \in [L]$ in the ideal case):

$$C_r := [P_{\ell_r, m_r}^\top, P_{\ell_{r+1}, m_r}^\top]^\top, \quad C_{r+1} := [P_{\ell_{r+1}, m_{r+1}}^\top, P_{\ell_{r+2}, m_{r+1}}^\top]^\top.$$

The top- K SVDs of \mathbf{C}_r and \mathbf{C}_{r+1} can be represented as follows:

$$\mathbf{C}_r = [\mathbf{U}_{\ell_r}^\top, \mathbf{U}_{\ell_{r+1}}^\top]^\top \boldsymbol{\Sigma}_r \mathbf{V}_{m_r}^\top, \quad \mathbf{C}_{r+1} = [\bar{\mathbf{U}}_{\ell_{r+1}}^\top, \bar{\mathbf{U}}_{\ell_{r+2}}^\top]^\top \boldsymbol{\Sigma}_{r+1} \mathbf{V}_{m_{r+1}}^\top. \quad (12)$$

Combining (11) and (12), and using the assumption that $\text{rank}(\mathbf{M}_\ell) = \text{rank}(\mathbf{B}) = K$ and $K \leq |\mathcal{S}_\ell|$ for every ℓ , the following equations hold:

$$\mathbf{U}_{\ell_r} = \mathbf{M}_{\ell_r}^\top \mathbf{G}_r, \quad \mathbf{U}_{\ell_{r+1}} = \mathbf{M}_{\ell_{r+1}}^\top \mathbf{G}_r, \quad (13a)$$

$$\bar{\mathbf{U}}_{\ell_{r+1}} = \mathbf{M}_{\ell_{r+1}}^\top \bar{\mathbf{G}}_{r+1}, \quad \bar{\mathbf{U}}_{\ell_{r+2}} = \mathbf{M}_{\ell_{r+2}}^\top \bar{\mathbf{G}}_{r+1}, \quad (13b)$$

where $\mathbf{G}_r \in \mathbb{R}^{K \times K}$ and $\bar{\mathbf{G}}_{r+1} \in \mathbb{R}^{K \times K}$ are certain nonsingular matrices. The equations in (13) imply that \mathbf{U}_{ℓ_r} , $\mathbf{U}_{\ell_{r+1}}$ and $\bar{\mathbf{U}}_{\ell_{r+2}}$ are the bases of $\text{range}(\mathbf{M}_{\ell_r}^\top)$, $\text{range}(\mathbf{M}_{\ell_{r+1}}^\top)$ and $\text{range}(\mathbf{M}_{\ell_{r+2}}^\top)$, respectively. Since $\mathbf{G}_r = \bar{\mathbf{G}}_{r+1}$ does not generally hold, the basis $\bar{\mathbf{U}}_{\ell_{r+2}}$ cannot be directly combined with the bases \mathbf{U}_{ℓ_r} and $\mathbf{U}_{\ell_{r+1}}$ to obtain $\text{range}([\mathbf{M}_{\ell_r}, \mathbf{M}_{\ell_{r+1}}, \mathbf{M}_{\ell_{r+2}}]^\top)$. Therefore, we are interested in obtaining the basis defined as below:

$$\mathbf{U}_{\ell_{r+2}} := \mathbf{M}_{\ell_{r+2}}^\top \mathbf{G}_r. \quad (14)$$

In order to identify $\mathbf{U}_{\ell_{r+2}}$ as defined in (14), we use the second equality in (13a) and the first equality in (13b) to construct the following:

$$\bar{\mathbf{U}}_{\ell_{r+1}}^\dagger \mathbf{U}_{\ell_{r+1}} = \bar{\mathbf{G}}_{r+1}^{-1} \mathbf{G}_r. \quad (15)$$

Combining the second equality in (13b) with (15), we have

$$\bar{\mathbf{U}}_{\ell_{r+2}} \bar{\mathbf{U}}_{\ell_{r+1}}^\dagger \mathbf{U}_{\ell_{r+1}} = (\mathbf{M}_{\ell_{r+2}}^\top \bar{\mathbf{G}}_{r+1}) (\bar{\mathbf{G}}_{r+1}^{-1} \mathbf{G}_r) = \mathbf{M}_{\ell_{r+2}}^\top \mathbf{G}_r.$$

Hence, the following holds:

$$\mathbf{U}_{\ell_{r+2}} = \bar{\mathbf{U}}_{\ell_{r+2}} \bar{\mathbf{U}}_{\ell_{r+1}}^\dagger \mathbf{U}_{\ell_{r+1}} = \mathbf{M}_{\ell_{r+2}}^\top \mathbf{G}_r, \quad (16)$$

where $\bar{\mathbf{U}}_{\ell_{r+2}}$ and $\bar{\mathbf{U}}_{\ell_{r+1}}$ are obtained from the top- K SVD of \mathbf{C}_{r+1} and $\mathbf{U}_{\ell_{r+1}}$ is obtained from the top- K SVD of \mathbf{C}_r .

Similarly, $\mathbf{U}_{\ell_{r-1}}$ can be identified using the top- K SVDs of \mathbf{C}_r and \mathbf{C}_{r-1} by the following:

$$\mathbf{U}_{\ell_{r-1}} = \bar{\mathbf{U}}_{\ell_{r-1}} \bar{\mathbf{U}}_{\ell_r}^\dagger \mathbf{U}_{\ell_r} = \mathbf{M}_{\ell_{r-1}}^\top \mathbf{G}_r, \quad (17)$$

where \mathbf{U}_{ℓ_r} is obtained from the top- K SVD of \mathbf{C}_r and $\bar{\mathbf{U}}_{\ell_{r-1}}$ and $\bar{\mathbf{U}}_{\ell_r}$ are obtained from the top- K SVD of $\mathbf{C}_{r-1} := [\mathbf{P}_{\ell_{r-1}, m_{r-1}}^\top, \mathbf{P}_{\ell_r, m_{r-1}}^\top]^\top$.

Algorithm 1 first applies top- K SVD for \mathbf{C}_T where $T = \lfloor L/2 \rfloor$ and the bases \mathbf{U}_{ℓ_T} and $\mathbf{U}_{\ell_{T+1}}$ are identified (Lines 2-3). By letting $\mathbf{G}_T = \mathbf{G}$, we thus obtain

$$\mathbf{U}_{\ell_T} = \mathbf{M}_{\ell_T}^\top \mathbf{G} \quad \text{and} \quad \mathbf{U}_{\ell_{T+1}} = \mathbf{M}_{\ell_{T+1}}^\top \mathbf{G}. \quad (18)$$

Next, we use induction to show how the iterations in Algorithm 1 (lines 5-10) identify $\mathbf{U}_{\ell_{T+2}}, \dots, \mathbf{U}_L$. The induction hypothesis is that before any iteration at $r = T+1, T+2, \dots, L-1$, the basis \mathbf{U}_{ℓ_r} is identified from the previous iteration such that $\mathbf{U}_{\ell_r} = \mathbf{M}_{\ell_r}^\top \mathbf{G}$. Note that the induction hypothesis holds true for $r = T+1$ from lines 2-3 of Algorithm 1 by performing top- K SVD of \mathbf{C}_T . From (16),

we have seen that given \mathbf{U}_{ℓ_r} , one can identify $\mathbf{U}_{\ell_{r+1}}$ using the matrices resulted from the top- K SVD of \mathbf{C}_r . Therefore, by induction, we can establish that Algorithm 1 identifies

$$\mathbf{U}_{\ell_r} = \mathbf{M}_{\ell_r}^\top \mathbf{G}, \text{ for every } r \in \{T+2, \dots, L\}. \quad (19)$$

Similarly, using induction via employing the results in (17) and (18), we can establish that lines 11-16 of Algorithm 1 identifies

$$\mathbf{U}_{\ell_r} = \mathbf{M}_{\ell_r}^\top \mathbf{G}, \text{ for every } r \in \{1, \dots, T-1\}. \quad (20)$$

Combining (18), (19), and (20), one can see that Algorithm 1 identifies $\widehat{\mathbf{U}} = [\mathbf{U}_1^\top, \mathbf{U}_2^\top, \dots, \mathbf{U}_L^\top]^\top$ such that $\text{range}(\widehat{\mathbf{U}}) = \text{range}([\mathbf{M}_1, \mathbf{M}_2, \dots, \mathbf{M}_L]^\top)$.

B Proof of Theorem 2

B.1 Estimation of the subspace

In Theorem 1, the subspace identifiability is established via successively applying the top- K SVD on $\mathbf{C}_r := [\mathbf{P}_{\ell_r, m_r}^\top, \mathbf{P}_{\ell_{r+1}, m_r}^\top]^\top$, i.e., $\mathbf{C}_r = [\overline{\mathbf{U}}_{\ell_r}^\top, \overline{\mathbf{U}}_{\ell_{r+1}}^\top]^\top \boldsymbol{\Sigma}_r \mathbf{V}_{m_r}^\top$. However, since \mathbf{C}_r is not observed in practice, Algorithm 1 performs the top- K SVD on its estimates $\widehat{\mathbf{C}}_r$, which is defined as $\widehat{\mathbf{C}}_r := [\mathbf{A}_{\ell_r, m_r}^\top, \mathbf{A}_{\ell_{r+1}, m_r}^\top]^\top$. The factors extracted from the top- K SVD of $\widehat{\mathbf{C}}_r$ are denoted as $\widehat{\mathbf{U}}_{\ell_r}$ and $\widehat{\mathbf{U}}_{\ell_{r+1}}$, which correspond to the ‘noiseless versions’ $\overline{\mathbf{U}}_{\ell_r}$ and $\overline{\mathbf{U}}_{\ell_{r+1}}$, respectively. To proceed, we invoke the following lemma to bound the estimation accuracy of $\widehat{\mathbf{U}}_{\ell_r}$ and $\widehat{\mathbf{U}}_{\ell_{r+1}}$.

Lemma 1 Denote $\sigma_1 := \max_{r \in [L-1]} \sigma_{\max}(\mathbf{C}_r)$ and $\sigma_K := \min_{r \in [L-1]} \sigma_{\min}(\mathbf{C}_r)$. Assume that

$$\text{rank}(\mathbf{C}_r) = K, \quad \|\widehat{\mathbf{C}}_r - \mathbf{C}_r\|_2 \leq \|\mathbf{C}_r\|_2. \quad (21)$$

Then, there exists an orthogonal matrix \mathbf{O}_r such that

$$\|\widehat{\mathbf{U}}_{\ell_r} - \overline{\mathbf{U}}_{\ell_r} \mathbf{O}_r\|_F \leq \frac{6\sqrt{2K}\sigma_1 \|\widehat{\mathbf{C}}_r - \mathbf{C}_r\|_2}{\sigma_K^2}. \quad (22)$$

In addition, $\|\widehat{\mathbf{U}}_{\ell_{r+1}} - \overline{\mathbf{U}}_{\ell_{r+1}} \mathbf{O}_r\|_F$ admits the same upper bound in (22).

The proof of the lemma is given in Sec. C in the supplemental material.

In order to utilize the bound in (22), we proceed to characterize the term $\|\widehat{\mathbf{C}}_r - \mathbf{C}_r\|_2$. To this end, we present the following lemma:

Lemma 2 Let $\rho := \max_{i, j \in [N]} P(i, j)$. Assume there exists a positive constant c_0 such that $L \leq \frac{4\rho N}{d}$ and $\rho \geq \frac{Lc_0 \log(3N/L)}{3N}$. Then, there exists another positive constant \tilde{c} (which is a function of c_0) such that

$$\|\widehat{\mathbf{C}}_r - \mathbf{C}_r\|_2 \leq \tilde{c} \sqrt{\rho N/L}, \quad \forall r \in [L-1] \quad (23)$$

holds with probability of at least $1 - \frac{L}{2N}$.

The proof of the lemma is given in Sec. D.

Since $\{\ell_r\}_{r=1}^L = [L]$ according to EQP, without loss of any generality (w.o.l.g.), in the following sections of the proof, we can fix $\ell_r = r$ for every r . Combining Lemma 1 and 2, the inequalities, i.e.,

$$\|\widehat{\mathbf{U}}_r - \overline{\mathbf{U}}_r \mathbf{O}_r\|_{\text{F}} \leq \phi \quad \text{and} \quad \|\widehat{\mathbf{U}}_{r+1} - \overline{\mathbf{U}}_{r+1} \mathbf{O}_r\|_{\text{F}} \leq \phi \quad (24)$$

hold with probability at least $1 - \frac{L}{N}$ where $\phi = \frac{6\tilde{c}\sqrt{2K\rho(N/L)}\sigma_1}{\sigma_K^2}$.

Algorithm 1 first estimates \mathbf{U}_T and \mathbf{U}_{T+1} by directly performing the top- K SVD to $\widehat{\mathbf{C}}_T = [\mathbf{A}_{T,m_T}^\top, \mathbf{A}_{T+1,m_T}^\top]^\top$. Recall that we use the notation $\mathbf{C}_T = [\mathbf{P}_{T,m_T}^\top, \mathbf{P}_{T+1,m_T}^\top]^\top = [\mathbf{U}_T^\top, \mathbf{U}_{T+1}^\top]^\top \boldsymbol{\Sigma}_T \mathbf{V}_{m_T}^\top$. Therefore, by (24) and denoting $\mathbf{O}_T := \mathbf{O}$, we have

$$\|\widehat{\mathbf{U}}_T - \mathbf{U}_T \mathbf{O}\|_{\text{F}} \leq \phi \quad \text{and} \quad \|\widehat{\mathbf{U}}_{T+1} - \mathbf{U}_{T+1} \mathbf{O}\|_{\text{F}} \leq \phi, \quad (25)$$

where $\widehat{\mathbf{U}}_T$ and $\widehat{\mathbf{U}}_{T+1}$ are the factors resulted from the top- K SVD of $\widehat{\mathbf{C}}_T$.

Next, the iterative steps (lines 5-10) in Algorithm 1 perform the below operation to estimate the basis \mathbf{U}_{r+1} for $r = T + 1, \dots, L$ (where $T = \lfloor L/2 \rfloor$):

$$\widehat{\mathbf{U}}_{r+1} = \widehat{\mathbf{U}}_{r+1} \widehat{\mathbf{U}}_r^\dagger \widehat{\mathbf{U}}_r. \quad (26)$$

In order to analyze $\widehat{\mathbf{U}}_{r+1}$, we will use the following three lemmas:

Lemma 3 *Under Assumption 2, there exists constants β_{\min} and β_{\max} such that for $r \in [L - 1]$, we have $\sigma_{\max}([\mathbf{M}_r, \mathbf{M}_{r+1}]) \leq \beta_{\max} = \sqrt{2K}\alpha_{\max}$, and $\sigma_{\min}([\mathbf{M}_r, \mathbf{M}_{r+1}]) \geq \beta_{\min} = \alpha_{\min}$.*

Lemma 4 *Let $\widehat{\mathbf{U}}_r$ denote the noisy estimate of $\overline{\mathbf{U}}_r \mathbf{O}_r$ obtained from the top- K SVD of $\widehat{\mathbf{C}}_r$. Suppose that Assumption 2 holds and $\|\widehat{\mathbf{U}}_r - \overline{\mathbf{U}}_r \mathbf{O}_r\|_2 \leq \frac{\alpha_{\min}}{2\beta_{\max}}$. Then, we have $\|\widehat{\mathbf{U}}_r^\dagger - (\overline{\mathbf{U}}_r \mathbf{O}_r)^\dagger\|_2 \leq \frac{2\sqrt{2}\beta_{\max}^2}{\alpha_{\min}^2} \|\widehat{\mathbf{U}}_r - (\overline{\mathbf{U}}_r \mathbf{O}_r)\|_2$.*

Lemma 5 *Consider the relation in (26). Suppose that Assumption 2 holds. Also assume that $\|\widehat{\mathbf{U}}_r - \overline{\mathbf{U}}_r \mathbf{O}_r\|_2 \leq \frac{\alpha_{\min}}{2\beta_{\max}}$ and $\|\widehat{\mathbf{U}}_{r+1} - \overline{\mathbf{U}}_{r+1} \mathbf{O}_r\|_2 \leq \frac{\alpha_{\min}}{2\beta_{\max}}$, then we have*

$$\begin{aligned} \|\widehat{\mathbf{U}}_{r+1} - \mathbf{U}_{r+1} \mathbf{O}\|_2 &\leq \frac{\beta_{\max}}{\alpha_{\min}} \frac{\alpha_{\max}}{\beta_{\min}} \|\widehat{\mathbf{U}}_{r+1} - \overline{\mathbf{U}}_{r+1} \mathbf{O}_r\|_2 + 2 \left(\frac{\alpha_{\max}}{\beta_{\min}} \right)^2 \|\widehat{\mathbf{U}}_r^\dagger - (\overline{\mathbf{U}}_r \mathbf{O}_r)^\dagger\|_2 \\ &\quad + 4 \frac{\beta_{\max}}{\alpha_{\min}} \frac{\alpha_{\max}}{\beta_{\min}} \|\widehat{\mathbf{U}}_r - \mathbf{U}_r \mathbf{O}\|_2. \end{aligned}$$

The proofs of Lemma 3-5 can be found Sec. E, Sec. F, and Sec. G of the supplemental material, respectively. Combining Lemma 3-5, we get

$$\begin{aligned} &\|\widehat{\mathbf{U}}_{r+1} - \mathbf{U}_{r+1} \mathbf{O}\|_2 \\ &\leq \bar{\kappa} \|\widehat{\mathbf{U}}_{r+1} - \overline{\mathbf{U}}_{r+1} \mathbf{O}_r\|_2 + 4\sqrt{2}\bar{\kappa}^2 \|\widehat{\mathbf{U}}_r - (\overline{\mathbf{U}}_r \mathbf{O}_r)\|_2 + 4\bar{\kappa} \|\widehat{\mathbf{U}}_r - \mathbf{U}_r \mathbf{O}\|_2, \end{aligned} \quad (27)$$

where $\bar{\kappa} := \frac{\beta_{\max}}{\alpha_{\min}} \frac{\alpha_{\max}}{\beta_{\min}} = \frac{\sqrt{2K}\alpha_{\max}}{\alpha_{\min}} \frac{\alpha_{\max}}{\alpha_{\min}} = \sqrt{2K}\gamma^2$.

Hence, we obtain the below set of inequalities with probability greater than $1 - \frac{L}{N}$:

$$\begin{aligned} \|\widehat{\mathbf{U}}_{r+1} - \mathbf{U}_{r+1}\mathbf{O}\|_F &\leq \sqrt{K}\|\widehat{\mathbf{U}}_{r+1} - \mathbf{U}_{r+1}\mathbf{O}\|_2 \\ &\leq \sqrt{K}\left(\bar{\kappa}\|\widehat{\mathbf{U}}_{r+1} - \bar{\mathbf{U}}_{r+1}\mathbf{O}_r\|_2 + 4\sqrt{2}\bar{\kappa}^2\|\widehat{\mathbf{U}}_r - (\bar{\mathbf{U}}_r\mathbf{O}_r)\|_2 + 4\bar{\kappa}\|\widehat{\mathbf{U}}_r - \mathbf{U}_r\mathbf{O}\|_2\right) \\ &\leq 5\sqrt{2K}\bar{\kappa}^2\phi + 4\bar{\kappa}\sqrt{K}\|\widehat{\mathbf{U}}_r - \mathbf{U}_r\mathbf{O}\|_F, \end{aligned}$$

where $\phi = \frac{6\tilde{c}\sqrt{2K\rho(N/L)\sigma_1}}{\sigma_K^2}$. The first inequality is obtained by using norm equivalence, the second inequality is obtained by applying (27) and the last inequality is by applying (24) and using the fact that $\bar{\kappa} \geq 1$.

By recursively applying the above result for any $r \in \{T+1, \dots, L-1\}$, we further have

$$\begin{aligned} \|\widehat{\mathbf{U}}_{r+1} - \mathbf{U}_{r+1}\mathbf{O}\|_F &\leq 5\sqrt{2K}\bar{\kappa}^2\phi + 4\sqrt{K}\bar{\kappa}\left(5\sqrt{2K}\bar{\kappa}^2\phi + 4\sqrt{K}\bar{\kappa}\dots\left(5\sqrt{2K}\bar{\kappa}^2\phi + 4\sqrt{K}\bar{\kappa}\|\widehat{\mathbf{U}}_{T+1} - \mathbf{U}_{T+1}\mathbf{O}\|_F\right)\right) \\ &\leq 5\sqrt{2K}\bar{\kappa}^2\phi + 4\sqrt{K}\bar{\kappa}\left(5\sqrt{2K}\bar{\kappa}^2\phi + 4\sqrt{K}\bar{\kappa}\dots\left(5\sqrt{2K}\bar{\kappa}^2\phi + 4\sqrt{K}\bar{\kappa}\phi\right)\right) \\ &= 5\sqrt{2K}\bar{\kappa}^2\phi\left(1 + 4\sqrt{K}\bar{\kappa} + (4\sqrt{K}\bar{\kappa})^2 + \dots + (4\sqrt{K}\bar{\kappa})^{r-T}\right), \end{aligned}$$

where we have applied (25) for obtaining the last inequality. By applying the geometric sum formula, for any $r \in \{T+1, \dots, L-1\}$, we have

$$\|\widehat{\mathbf{U}}_{r+1} - \mathbf{U}_{r+1}\mathbf{O}\|_F \leq \frac{5\sqrt{2K}\bar{\kappa}^2\phi\left((4\sqrt{K}\bar{\kappa})^{r-T+1} - 1\right)}{4\sqrt{K}\bar{\kappa} - 1} \leq \frac{5\sqrt{2K}\bar{\kappa}^2\phi(4\sqrt{K}\bar{\kappa})^{r-T+1}}{4\sqrt{K}\bar{\kappa} - 1}. \quad (28)$$

Following the same derivation, one can show that for $r = 2, \dots, T$, we have

$$\|\widehat{\mathbf{U}}_{r-1} - \mathbf{U}_{r-1}\mathbf{O}\|_F \leq \frac{5\sqrt{2K}\bar{\kappa}^2\phi(4\sqrt{K}\bar{\kappa})^{T-r+2}}{4\sqrt{K}\bar{\kappa} - 1}. \quad (29)$$

Consequently, we get

$$\begin{aligned} \|\widehat{\mathbf{U}} - \mathbf{U}\mathbf{O}\|_F &\leq \sum_{r=1}^L \|\widehat{\mathbf{U}}_r - \mathbf{U}_r\mathbf{O}\|_F \\ &= \sum_{r=1}^{T-1} \|\widehat{\mathbf{U}}_r - \mathbf{U}_r\mathbf{O}\|_F + \|\widehat{\mathbf{U}}_T - \mathbf{U}_T\mathbf{O}\|_F + \|\widehat{\mathbf{U}}_{T+1} - \mathbf{U}_{T+1}\mathbf{O}\|_F + \sum_{r=T+2}^L \|\widehat{\mathbf{U}}_r - \mathbf{U}_r\mathbf{O}\|_F \\ &\leq \frac{5\sqrt{2K}\bar{\kappa}^2\phi(4\sqrt{K}\bar{\kappa})^{T+1}}{(4\sqrt{K}\bar{\kappa} - 1)^2} + \frac{5\sqrt{2K}\bar{\kappa}^2\phi(4\sqrt{K}\bar{\kappa})^{T+1}}{(4\sqrt{K}\bar{\kappa} - 1)^2} = \frac{10\sqrt{2K}\bar{\kappa}^2\phi(4\sqrt{K}\bar{\kappa})^{L/2+1}}{(4\sqrt{K}\bar{\kappa} - 1)^2}, \end{aligned}$$

where the first inequality is by the triangle inequality, the second inequality is obtained by (25), (28), (29), and by the geometric sum formula.

Substituting $\phi = \frac{6\tilde{c}\sqrt{2K\rho(N/L)\sigma_1}}{\sigma_K^2}$ into the above result, we have the following result with probability at least $1 - L(L-1)/N$:

$$\|\widehat{\mathbf{U}} - \mathbf{U}\mathbf{O}\|_F \leq \frac{15K\tilde{c}\bar{\kappa}^2(4\sqrt{K}\bar{\kappa})^{(L/2+1)}\sigma_1\sqrt{\rho(N/L)}}{2(\sqrt{K}\bar{\kappa} - 1)^2\sigma_K^2}. \quad (30)$$

Note that we have applied union bound to reach the probability $1 - L(L - 1)/N$, since the bound (24) derived from Lemma 2 are invoked for every $r \in [L - 1]$. Next, we bound σ_1 and σ_K using the following lemma:

Lemma 6 *Assume that the columns of \mathbf{M} are generated from any continuous distribution and there exist positive constants c and C , where $c \leq C$ depending only on distribution of the columns of \mathbf{M} . Also assume that $(N/L) \geq \frac{4}{c} \log(NK/L)$. Then, the following holds true with probability at least $1 - (3L(L - 1)/N)$:*

$$\sigma_K \geq \sqrt{2}\sigma_{\min}(\mathbf{B})c(N/L), \quad (31)$$

$$\sigma_1 \leq \sqrt{2}\sigma_{\max}(\mathbf{B})C(N/L). \quad (32)$$

The proof can be found in Sec. I.

Applying Lemma 6 in (30) and substituting $\bar{\kappa} = \sqrt{2K}\gamma^2$, we get the following with probability at least $1 - (4L(L - 1)/N)$:

$$\|\widehat{\mathbf{U}} - \mathbf{U}\mathbf{O}\|_F = \frac{15K^2\tilde{c}C\gamma^4(4\sqrt{2}K\gamma^2)^{(L/2+1)}\kappa(\mathbf{B})\sqrt{\rho}}{c^2\sigma_{\min}(\mathbf{B})(\sqrt{2}K\gamma^2 - 1)^2\sqrt{2(N/L)}} := \zeta. \quad (33)$$

To make the above derivation legitimate, we need the assumptions in Lemma 1-6 hold true. The assumptions on \mathbf{C}_r in Lemma 1 given by the equalities in (21) are satisfied if

$$\text{rank}(\mathbf{M}_r) = \text{rank}(\mathbf{B}) = K, \quad \forall r \in [L] \quad \text{and} \quad (34)$$

$$\tilde{c}\sqrt{\rho N/L} \leq \sigma_K. \quad (35)$$

Using (31), The condition (35) can be further written as

$$N/L \geq \frac{\tilde{c}^2\rho}{2\sigma_{\min}^2(\mathbf{B})c^2}. \quad (36)$$

The assumption in Lemma 4 and Lemma 5 can be written as:

$$\phi = \frac{6\tilde{c}\sqrt{2K\rho(N/L)}\sigma_1}{\sigma_K^2} \leq \frac{6\tilde{c}C\kappa(\mathbf{B})\sqrt{K\rho}}{c^2\sigma_{\min}(\mathbf{B})\sqrt{(N/L)}} \leq \frac{\alpha_{\min}}{2\beta_{\max}} = \frac{\alpha_{\min}}{2\sqrt{2K}\alpha_{\max}} = \frac{1}{2\sqrt{2K}\gamma},$$

where we have utilized Lemma 6 to obtain the first inequality and Lemma 3 to obtain the second equality. Hence, we obtain the condition such that

$$N/L \geq \frac{(6\sqrt{2}\tilde{c}C)^2\kappa^2(\mathbf{B})K^2\rho\gamma^2}{c^4\sigma_{\min}^2(\mathbf{B})}. \quad (37)$$

We can see that the condition in (36) is satisfied if (37) holds.

Also, the below conditions from Lemma 2 and 6 have to be satisfied:

$$L \leq \frac{4\rho N}{d}, \quad \rho \geq \frac{Lc_0 \log(3N/L)}{3N} \quad (38a)$$

$$(N/L) \geq \frac{4}{c} \log(NK/L). \quad (38b)$$

Hence, if the conditions (34), (37), and (38) are satisfied, the bound given by (33) holds true with probability of at least $1 - (4L(L - 1)/N)$.

B.2 Estimation of the membership matrix

Note that in the $\mathbf{A} = \mathbf{P}$ case, $\text{range}(\mathbf{U}) = \text{range}(\mathbf{M}^\top)$. Therefore, there exists a nonsingular matrix $\mathbf{G} \in \mathbb{R}^{K \times K}$ such that $\mathbf{U} = \mathbf{M}^\top \mathbf{G}$. In the binary observation case, in order to estimate the membership matrix \mathbf{M} , Algorithm 1 applies SPA to the estimated $\widehat{\mathbf{U}}$. To analyze this step, we start by considering the following noisy NMF model:

$$\widehat{\mathbf{U}}^\top = \mathbf{O}^\top \mathbf{G}^\top \mathbf{M} + \mathbf{N}, \quad (39)$$

where \mathbf{O} is the orthogonal matrix, \mathbf{M} satisfies simplex constraints, i.e., $\mathbf{M} \geq \mathbf{0}, \mathbf{1}^\top \mathbf{M} = \mathbf{1}^\top$ and $\mathbf{N} \in \mathbb{R}^{K \times N}$ is the noise matrix, whose Euclidean norm upper bound was analyzed in the previous subsection. From the noisy observation $\widehat{\mathbf{U}}$, one can get an estimate for \mathbf{M} employing SPA. To see this, we consider the following lemma:

Lemma 7 [34] *Let $\mu > 0, \varepsilon > 0$, and assume that the columns of $\mathbf{M} \in \mathbb{R}^{K \times N}$ are sampled from the probability simplex uniformly at random. If the number of columns satisfies*

$$N = \Omega \left(\frac{\varepsilon^{-2(K-1)}}{K} \log \left(\frac{K}{\mu} \right) \right), \quad (40)$$

then, with probability of at least $1 - \mu$, there exist columns of \mathbf{M} indexed by n_1, \dots, n_K such that

$$\|\mathbf{M}(:, n_k) - \mathbf{e}_k\|_2 \leq \varepsilon, \quad k = 1, \dots, K. \quad (41)$$

Eq. (41) means that \mathbf{M} approximately satisfies the separability condition that is widely used in SSMF [32, 33]. In the context of community detection, the existence of the set $\{n_1, \dots, n_K\}$ in Lemma 7 means that there exists a set of nodes who are mostly associated with a single cluster, i.e., the pure/anchor nodes. The existence of anchor nodes makes applying separability-based SSMF methods to extract \mathbf{M} viable. Using the noise robustness analysis of SPA in [33], we show the following:

Lemma 8 *Consider the noisy model in (39) and assume that $\|\mathbf{N}\|_F \leq \zeta$ and that \mathbf{M} satisfies (41). Also suppose that Assumption 2 holds, and that*

$$\zeta \leq \frac{1}{4\sqrt{2}K\alpha_{\max}\tilde{\kappa}(\mathbf{M})} \quad \text{and} \quad \varepsilon \leq \frac{1}{4\sqrt{2}K\gamma\tilde{\kappa}(\mathbf{M})}. \quad (42)$$

Then, Algorithm 1 outputs $\widehat{\mathbf{M}}$ such that $\min_{\mathbf{M}} \|\widehat{\mathbf{M}} - \mathbf{M}\|_F \leq \sigma_{\max}(\mathbf{M})\sqrt{2}K\gamma\tilde{\kappa}(\mathbf{M})(3\varepsilon + 4\zeta)$, where $\tilde{\kappa}(\mathbf{M}) = 1 + 160K\gamma^2$ and $\gamma = \alpha_{\max}/\alpha_{\min}$.

The proof is provided in Section J.

By substituting the value of ζ given by (33), the condition on ζ in (42) can be re-written as:

$$N/L \geq \frac{(30K^3\tilde{c}C\gamma^4\kappa(\mathbf{B})\tilde{\kappa}(\mathbf{M})\alpha_{\max})^2\rho(4\sqrt{2}K\gamma^2)^{L+2}}{(c^2\sigma_{\min}(\mathbf{B})(K\gamma^2 - 1)^2)}. \quad (43)$$

Note that we derived another condition on N given by (37), which is satisfied if the above condition on N holds true. Hence, if the conditions (40) and (43) are satisfied together with (34) and (38), the bound given by Theorem 2 holds true with probability of at least $1 - (4L(L-1)/N)$.

C Proof of Lemma 1

We invoke the following lemma from [43] to characterize the estimation accuracy of the factors resulting from the top- K SVD of $\widehat{\mathbf{C}}_r$:

Lemma 9 [43] *Let $\mathbf{C} \in \mathbb{R}^{m \times n}$ and $\widehat{\mathbf{C}} \in \mathbb{R}^{m \times n}$ have singular values $\alpha_1 \geq \alpha_2 \geq \dots \geq \alpha_{\min(m,n)}$ and $\widehat{\alpha}_1 \geq \widehat{\alpha}_2 \geq \dots \geq \widehat{\alpha}_{\min(m,n)}$, respectively. Fix $1 \leq t \leq s \leq \text{rank}(\mathbf{C})$ and assume that $\min(\alpha_{t-1}^2 - \alpha_t^2, \alpha_s^2 - \alpha_{s+1}^2) > 0$, where $\alpha_0^2 := \infty$ and $\alpha_{\text{rank}(\mathbf{C})+1} := 0$. Let $q := s - t + 1$ and let $\mathbf{U} = [\mathbf{u}_t, \mathbf{u}_{t+1}, \dots, \mathbf{u}_s] \in \mathbb{R}^{m \times q}$ and $\widehat{\mathbf{U}} = [\widehat{\mathbf{u}}_t, \widehat{\mathbf{u}}_{t+1}, \dots, \widehat{\mathbf{u}}_s] \in \mathbb{R}^{m \times q}$ have orthonormal columns satisfying $\mathbf{C}^\top \mathbf{u}_j = \alpha_j \mathbf{v}_j$ and $\widehat{\mathbf{C}}^\top \widehat{\mathbf{u}}_j = \widehat{\alpha}_j \widehat{\mathbf{v}}_j$ for $j = t, t+1, \dots, s$ and let $\mathbf{V} = [\mathbf{v}_t, \mathbf{v}_{t+1}, \dots, \mathbf{v}_s] \in \mathbb{R}^{n \times q}$ and $\widehat{\mathbf{V}} = [\widehat{\mathbf{v}}_t, \widehat{\mathbf{v}}_{t+1}, \dots, \widehat{\mathbf{v}}_s] \in \mathbb{R}^{n \times q}$ have orthonormal columns satisfying $\mathbf{C} \mathbf{v}_j = \alpha_j \mathbf{u}_j$ and $\widehat{\mathbf{C}} \widehat{\mathbf{v}}_j = \widehat{\alpha}_j \widehat{\mathbf{u}}_j$ for $j = t, t+1, \dots, s$. Then there exists an orthogonal matrix $\mathbf{O} \in \mathbb{R}^{q \times q}$ such that*

$$\|\widehat{\mathbf{U}} - \mathbf{U} \mathbf{O}\|_F \leq \frac{2^{3/2}(2\alpha_1 + \|\widehat{\mathbf{C}} - \mathbf{C}\|_2) \min(q^{1/2} \|\widehat{\mathbf{C}} - \mathbf{C}\|_2, \|\widehat{\mathbf{C}} - \mathbf{C}\|_F)}{\min(\alpha_{t-1}^2 - \alpha_t^2, \alpha_s^2 - \alpha_{s+1}^2)} \quad (44)$$

and the same upper bound holds for $\|\widehat{\mathbf{V}} - \mathbf{V} \mathbf{O}\|_F$.

By letting $t = 1$ and $s = K$, using the assumption that $\text{rank}(\mathbf{C}_r) = K$ and applying Lemma 9, we have

$$\begin{aligned} \|\widehat{\mathbf{U}}_{\ell_r} - \overline{\mathbf{U}}_{\ell_r} \mathbf{O}_r\|_F &\leq \frac{2^{3/2}(2\sigma_{\max}(\mathbf{C}_r) + \|\widehat{\mathbf{C}}_r - \mathbf{C}_r\|_2) \min(\sqrt{K} \|\widehat{\mathbf{C}}_r - \mathbf{C}_r\|_2, \|\widehat{\mathbf{C}}_r - \mathbf{C}_r\|_F)}{\sigma_{\min}(\mathbf{C}_r)^2} \\ &= \frac{2^{3/2} \sqrt{K} (2\sigma_{\max}(\mathbf{C}_r) + \|\widehat{\mathbf{C}}_r - \mathbf{C}_r\|_2) \|\widehat{\mathbf{C}}_r - \mathbf{C}_r\|_2}{\sigma_{\min}(\mathbf{C}_r)^2} \\ &\leq \frac{2^{3/2} \sqrt{K} 3\sigma_{\max}(\mathbf{C}_r) \|\widehat{\mathbf{C}}_r - \mathbf{C}_r\|_2}{\sigma_{\min}(\mathbf{C}_r)^2}, \end{aligned}$$

where $\mathbf{O}_r \in \mathbb{R}^{K \times K}$ is orthogonal, the first equality is due to the fact that for any matrix \mathbf{X} of rank at least K , $\|\mathbf{X}\|_F \leq \sqrt{\text{rank}(\mathbf{X})} \|\mathbf{X}\|_2$ and $\text{rank}(\mathbf{X}) \geq K$ and the last inequality by using the assumption that $\|\widehat{\mathbf{C}}_r - \mathbf{C}_r\|_2 \leq \|\mathbf{C}_r\|_2 = \sigma_{\max}(\mathbf{C}_r)$.

Therefore, using the defined σ_1 and σ_K , we have for any $r \in [L-1]$,

$$\|\widehat{\mathbf{U}}_{\ell_r} - \overline{\mathbf{U}}_{\ell_r} \mathbf{O}_r\|_F \leq \frac{6\sqrt{2K} \sigma_1 \|\widehat{\mathbf{C}}_r - \mathbf{C}_r\|_2}{\sigma_K^2}. \quad (45)$$

Note that upper bound in (45) is valid for $\|\widehat{\mathbf{U}}_{\ell_{r+1}} - \overline{\mathbf{U}}_{\ell_{r+1}} \mathbf{O}_r\|_F$ as well.

D Proof of Lemma 2

Consider the below lemma:

Lemma 10 [44] *Let $\mathbf{A} \in \mathbb{R}^{N \times N}$ be the symmetric binary adjacency matrix of a random graph on N nodes in which the edges $\mathbf{A}(i, j)$ occur independently. Let $\overline{\mathbf{P}}$ be a matrix of size $N \times N$ such that the entries $\overline{\mathbf{P}}(i, j) \in [0, 1]$. Assume that $\mathbf{A}(i, j) \sim \text{Bernoulli}(\overline{\mathbf{P}}(i, j))$ for $i < j$, $\mathbf{A}(j, i) = \mathbf{A}(i, j)$*

for $j > i$ and $\mathbf{A}(i, i) = 0$ for every $i \in [N]$. Set $\mathbb{E}[\mathbf{A}] = \bar{\mathbf{P}}$ and assume that $d \geq \max(\rho N, c_0 \log N)$ where $c_0 > 0$. Then, for any $t > 0$, there exists a constant $c_t = c(t, c_0)$ such that

$$\|\mathbf{A} - \bar{\mathbf{P}}\|_2 \leq c_t \sqrt{d},$$

with probability greater than $1 - N^{-t}$.

To utilize Lemma 10 in our case, we analyze diagonal pattern (rightmost pattern in Fig. 1) and nondiagonal patterns (for e.g., the first and second pattern in Fig. 1) of EQP separately. For the diagonal pattern where $\ell_r = r$ and $\ell_{r+1} = m_r = r + 1$ for every r , we consider the below sub-adjacency matrix for any $r \in [L - 1]$:

$$\tilde{\mathbf{A}}_r = \begin{bmatrix} \mathbf{A}_{r,r} & \mathbf{A}_{r,r+1} \\ \mathbf{A}_{r+1,r} & \mathbf{A}_{r+1,r+1} \end{bmatrix},$$

where $\tilde{\mathbf{A}}_r \in \mathbb{R}^{2N/L \times 2N/L}$.

Now, let us define

$$\tilde{\mathbf{P}}_r = \begin{bmatrix} \mathbf{P}_{r,r} & \mathbf{P}_{r,r+1} \\ \mathbf{P}_{r+1,r} & \mathbf{P}_{r+1,r+1} \end{bmatrix}.$$

It can be noted that $\mathbb{E}[\tilde{\mathbf{A}}_r] = \tilde{\mathbf{P}}_r - \text{diag}(\tilde{\mathbf{P}}_r)$. Denoting $\bar{\mathbf{P}}_r := \tilde{\mathbf{P}}_r - \text{diag}(\tilde{\mathbf{P}}_r)$ and $\rho := \max_{i,j \in [N]} \mathbf{P}(i, j)$, we have

$$\begin{aligned} \|\tilde{\mathbf{A}}_r - \tilde{\mathbf{P}}_r\|_2 &= \|\tilde{\mathbf{A}}_r - \bar{\mathbf{P}}_r + \bar{\mathbf{P}}_r - \tilde{\mathbf{P}}_r\|_2 = \|\tilde{\mathbf{A}}_r - \bar{\mathbf{P}}_r - \text{diag}(\tilde{\mathbf{P}}_r)\|_2 \\ &\leq \|\tilde{\mathbf{A}}_r - \bar{\mathbf{P}}_r\|_2 + \|\text{diag}(\tilde{\mathbf{P}}_r)\|_2 \\ &\leq \|\tilde{\mathbf{A}}_r - \bar{\mathbf{P}}_r\|_2 + \max_i \tilde{\mathbf{P}}_r(i, i) \\ &\leq \|\tilde{\mathbf{A}}_r - \bar{\mathbf{P}}_r\|_2 + \rho. \end{aligned} \tag{46}$$

In order to bound the first term $\|\tilde{\mathbf{A}}_r - \bar{\mathbf{P}}_r\|_2$, we can utilize Lemma 10. Hence, by assuming

$$d \geq \max\left(\frac{2\rho N}{L}, c_0 \log(2N/L)\right), \tag{47}$$

we apply Lemma 10 and (46) and obtain $\|\tilde{\mathbf{A}}_r - \tilde{\mathbf{P}}_r\|_2 \leq c_t \sqrt{d} + \rho$ with probability greater than $1 - (2N/L)^{-t}$. Next, we will rewrite the condition (47) in a simpler form. Suppose

$$\frac{2\rho N}{L} \geq c_0 \log(2N/L), \tag{48}$$

then the condition (47) becomes $d \geq \frac{2\rho N}{L}$. If we choose L to be small enough, then we can satisfy this condition on d , i.e., if we have

$$L \leq \frac{4\rho N}{d}, \tag{49}$$

then the condition $d \geq \frac{2\rho N}{L}$ gets automatically satisfied. Therefore, by using the assumptions (48)-(49) and fixing $t = 1$, we can apply Lemma 10 to obtain

$$\begin{aligned} \|\tilde{\mathbf{A}}_r - \tilde{\mathbf{P}}_r\|_2 &\leq c_1 \sqrt{d} + \rho \\ &\leq 2c_1 \sqrt{\rho N/L} + \rho \\ &\leq (2c_1 + 1) \sqrt{\rho N/L} \end{aligned} \tag{50}$$

with probability at least $1 - (2N/L)^{-1}$. In the above, the first inequality is by using the relation (46), the second inequality is by employing the assumed bound on L given in (49) and the third inequality is by using the fact that $\rho \leq 1$.

Then, we have

$$\begin{aligned} \|\widehat{\mathbf{C}}_r - \mathbf{C}_r\|_2 &= \left\| [\mathbf{A}_{r,r+1}^\top, \mathbf{A}_{r+1,r+1}^\top]^\top - [\mathbf{P}_{r,r+1}^\top, \mathbf{P}_{r+1,r+1}^\top]^\top \right\|_2 \\ &\leq \|\widetilde{\mathbf{A}}_r - \widetilde{\mathbf{P}}_r\|_2 \\ &\leq (2c_1 + 1)\sqrt{\rho N/L} \end{aligned} \quad (51)$$

holds with probability greater than $1 - (2N/L)^{-1}$, where we have applied (50) to obtain the last inequality.

In order to apply Lemma 10 for non-diagonal patterns in EQP, we start by defining \mathbf{A}_r^* and \mathbf{P}_r^* in the following way:

$$\mathbf{A}_r^* = \begin{bmatrix} \mathbf{0} & \mathbf{0} & \mathbf{A}_{\ell_r, m_r} \\ \mathbf{0} & \mathbf{0} & \mathbf{A}_{\ell_{r+1}, m_r} \\ \mathbf{A}_{\ell_r, m_r}^\top & \mathbf{A}_{\ell_{r+1}, m_r}^\top & \mathbf{0} \end{bmatrix}, \quad \mathbf{P}_r^* = \begin{bmatrix} \mathbf{0} & \mathbf{0} & \mathbf{P}_{\ell_r, m_r} \\ \mathbf{0} & \mathbf{0} & \mathbf{P}_{\ell_{r+1}, m_r} \\ \mathbf{P}_{\ell_r, m_r}^\top & \mathbf{P}_{\ell_{r+1}, m_r}^\top & \mathbf{0} \end{bmatrix}$$

where $\mathbf{0}$ represents a zero matrix which is of size $N/L \times N/L$. With this definition, we can see that $\mathbf{A}_r^*(i, j) \sim \text{Bernoulli}(\mathbf{P}_r^*(i, j))$ for $i < j$, $\mathbf{A}_r^*(j, i) = \mathbf{A}_r^*(i, j)$ for $j > i$, $\mathbf{A}_r^*(i, i) = 0$ for every i and $\mathbb{E}[\mathbf{A}_r^*] = \mathbf{P}_r^*$. Therefore, we can apply Lemma 10 by fixing $t = 1$ to result in

$$\|\mathbf{A}_r^* - \mathbf{P}_r^*\|_2 \leq c_1 \sqrt{d}, \quad (52)$$

with probability greater than $1 - (3N/L)^{-1}$. Similar as before, we can derive the conditions in order to obtain (52). It can be easily shown that the sufficient conditions to be satisfied are

$$\frac{3\rho N}{L} \geq c_0 \log(3N/L), \quad L \leq \frac{6\rho N}{d}. \quad (53)$$

Then, for non-diagonal EQP patterns, we have

$$\begin{aligned} \|\widehat{\mathbf{C}}_r - \mathbf{C}_r\|_2 &= \left\| [\mathbf{A}_{\ell_r, m_r}^\top, \mathbf{A}_{\ell_{r+1}, m_r}^\top]^\top - [\mathbf{P}_{\ell_r, m_r}^\top, \mathbf{P}_{\ell_{r+1}, m_r}^\top]^\top \right\|_2 \\ &\leq \|\mathbf{A}_r^* - \mathbf{P}_r^*\|_2 \\ &\leq c_1 \sqrt{d} \leq \sqrt{6}c_1 \sqrt{\rho N/L}, \end{aligned} \quad (54)$$

where we obtained the last inequality by applying the assumed bound on L as given by the second condition in (53).

Hence, from (51) and (54), we can see that $\|\widehat{\mathbf{C}}_r - \mathbf{C}_r\|_2$ is bounded for any patterns in EQP with probability of at least $1 - (2N/L)^{-1}$ if the below conditions are satisfied.

$$\frac{3\rho N}{L} \geq c_0 \log(3N/L), \quad L \leq \frac{4\rho N}{d}.$$

E Proof of Lemma 3

Consider the below relation for any $r \in [L - 1]$:

$$\begin{aligned}\sigma_{\max}^2([\mathbf{M}_r, \mathbf{M}_{r+1}]) &= \|[\mathbf{M}_r, \mathbf{M}_{r+1}]\|_2^2 \leq \|[\mathbf{M}_r, \mathbf{M}_{r+1}]\|_{\mathbb{F}}^2 \\ &= \|\mathbf{M}_r\|_{\mathbb{F}}^2 + \|\mathbf{M}_{r+1}\|_{\mathbb{F}}^2 \leq K\|\mathbf{M}_r\|_2^2 + K\|\mathbf{M}_{r+1}\|_2^2 \leq 2K\alpha_{\max}^2,\end{aligned}$$

where we have utilized the norm equivalence for the first and second inequalities and applied Assumption 2 for the last inequality. Hence, we have

$$\sigma_{\max}([\mathbf{M}_r, \mathbf{M}_{r+1}]) \leq \sqrt{2K}\alpha_{\max} := \beta_{\max}.$$

Next, consider the below for any vector $\mathbf{x} \in \mathbb{R}^K$ such that $\|\mathbf{x}\|_2 = 1$:

$$\begin{aligned}\|[\mathbf{M}_r, \mathbf{M}_{r+1}]^\top \mathbf{x}\|_2^2 &= \|\mathbf{M}_r^\top \mathbf{x}\|_2^2 + \|\mathbf{M}_{r+1}^\top \mathbf{x}\|_2^2 \\ \implies \min_{\mathbf{x}} \|[\mathbf{M}_r, \mathbf{M}_{r+1}]^\top \mathbf{x}\|_2^2 &= \min_{\mathbf{x}} \|\mathbf{M}_r^\top \mathbf{x}\|_2^2 + \min_{\mathbf{x}} \|\mathbf{M}_{r+1}^\top \mathbf{x}\|_2^2 \\ \implies \min_{\mathbf{x}} \|[\mathbf{M}_r, \mathbf{M}_{r+1}]^\top \mathbf{x}\|_2^2 &\geq \min_{\mathbf{x}} \|\mathbf{M}_r^\top \mathbf{x}\|_2^2 \\ \implies \sigma_{\min}([\mathbf{M}_r, \mathbf{M}_{r+1}]) &\geq \sigma_{\min}(\mathbf{M}_r) \geq \alpha_{\min} := \beta_{\min},\end{aligned}$$

where we have utilized Assumption 2 for the last inequality.

F Proof of Lemma 4

We utilize the following classic result to characterize the pseudo-inverse:

Lemma 11 [45] *Consider any matrices $\mathbf{A}, \mathbf{B}, \mathbf{E} \in \mathbb{R}^{m \times n}$ such that $\mathbf{B} = \mathbf{A} + \mathbf{E}$. Suppose $\text{rank}(\mathbf{B}) = \text{rank}(\mathbf{A})$. Then, we have*

$$\|\mathbf{B}^\dagger - \mathbf{A}^\dagger\|_2 \leq \sqrt{2}\|\mathbf{A}^\dagger\|_2\|\mathbf{B}^\dagger\|_2\|\mathbf{E}\|_2.$$

By fixing $\mathbf{B} := \widehat{\mathbf{U}}_r^\dagger$ and $\mathbf{A} = (\overline{\mathbf{U}}_r \mathbf{O}_r)^\dagger$, we can apply Lemma 11 to obtain

$$\|\widehat{\mathbf{U}}_r^\dagger - (\overline{\mathbf{U}}_r \mathbf{O}_r)^\dagger\|_2 \leq \sqrt{2}\|(\overline{\mathbf{U}}_r \mathbf{O}_r)^\dagger\|_2\|\widehat{\mathbf{U}}_r^\dagger\|_2\|\widehat{\mathbf{U}}_r - (\overline{\mathbf{U}}_r \mathbf{O}_r)\|_2. \quad (55)$$

Regarding the first term in the R.H.S. of the above equation, we have

$$\|(\overline{\mathbf{U}}_r \mathbf{O}_r)^\dagger\|_2 = \sigma_{\max}((\overline{\mathbf{U}}_r \mathbf{O}_r)^\dagger) = \frac{1}{\sigma_{\min}(\overline{\mathbf{U}}_r \mathbf{O}_r)} = \frac{1}{\sigma_{\min}(\overline{\mathbf{U}}_r)}, \quad (56)$$

where the last equality is due to the orthogonality of \mathbf{O}_r .

Similarly, we have

$$\|\widehat{\mathbf{U}}_r^\dagger\|_2 = \sigma_{\max}(\widehat{\mathbf{U}}_r^\dagger) = \frac{1}{\sigma_{\min}(\widehat{\mathbf{U}}_r)}. \quad (57)$$

To proceed, we aim to get a lower bound for $\sigma_{\min}(\widehat{\mathbf{U}}_r)$. For this, we have the following result:

Lemma 12 *The below relation holds true if $\|\widehat{\mathbf{U}}_r - \overline{\mathbf{U}}_r \mathbf{O}_r\|_2 \leq \sigma_{\min}(\overline{\mathbf{U}}_r)/2$:*

$$\sigma_{\min}(\widehat{\mathbf{U}}_r) \geq \sigma_{\min}(\overline{\mathbf{U}}_r)/2.$$

Proof 1 *Consider the below set of relations for any vector $\mathbf{x} \in \mathbb{R}^K$ satisfying $\|\mathbf{x}\| = 1$:*

$$\begin{aligned} \|\widehat{\mathbf{U}}_r \mathbf{x}\|_2 &= \|\overline{\mathbf{U}}_r \mathbf{O}_r \mathbf{x} + (\widehat{\mathbf{U}}_r - \overline{\mathbf{U}}_r \mathbf{O}_r) \mathbf{x}\|_2 \\ &\geq \|\overline{\mathbf{U}}_r \mathbf{O}_r \mathbf{x}\|_2 - \|(\widehat{\mathbf{U}}_r - \overline{\mathbf{U}}_r \mathbf{O}_r) \mathbf{x}\|_2, \\ \implies \min_{\mathbf{x}} \|\widehat{\mathbf{U}}_r \mathbf{x}\|_2 &\geq \min_{\mathbf{x}} \|\overline{\mathbf{U}}_r \mathbf{O}_r \mathbf{x}\|_2 - \max_{\mathbf{x}} \|(\widehat{\mathbf{U}}_r - \overline{\mathbf{U}}_r \mathbf{O}_r) \mathbf{x}\|_2, \\ \implies \sigma_{\min}(\widehat{\mathbf{U}}_r) &\geq \sigma_{\min}(\overline{\mathbf{U}}_r) - \|\widehat{\mathbf{U}}_r - \overline{\mathbf{U}}_r \mathbf{O}_r\|_2, \end{aligned}$$

where the first inequality is by applying the triangle inequality.

Using the assumption that $\|\widehat{\mathbf{U}}_r - \overline{\mathbf{U}}_r \mathbf{O}_r\|_2 \leq \sigma_{\min}(\overline{\mathbf{U}}_r)/2$, we get $\sigma_{\min}(\widehat{\mathbf{U}}_r) \geq \sigma_{\min}(\overline{\mathbf{U}}_r)/2$.

Applying (56), (57) and Lemma 12 in (55), we get

$$\|\widehat{\mathbf{U}}_r^\dagger - (\overline{\mathbf{U}}_r \mathbf{O}_r)^\dagger\|_2 \leq \frac{2\sqrt{2}}{\sigma_{\min}^2(\overline{\mathbf{U}}_r)} \|\widehat{\mathbf{U}}_r - (\overline{\mathbf{U}}_r \mathbf{O}_r)\|_2. \quad (58)$$

The final step is to characterize $\sigma_{\min}(\overline{\mathbf{U}}_r)$. For this, we utilize the following result:

Lemma 13 *Suppose that Assumption 2 holds true. Then, for every r , we have*

$$\begin{aligned} \sigma_{\min}(\overline{\mathbf{U}}_r) &\geq \frac{\sigma_{\min}(\mathbf{M}_r)}{\sigma_{\max}([\mathbf{M}_r, \mathbf{M}_{r+1}])} = \frac{\alpha_{\min}}{\beta_{\max}}, \\ \sigma_{\max}(\overline{\mathbf{U}}_r) &\leq \frac{\sigma_{\max}(\mathbf{M}_r)}{\sigma_{\min}([\mathbf{M}_r, \mathbf{M}_{r+1}])} = \frac{\alpha_{\max}}{\beta_{\min}}. \end{aligned}$$

Proof 2 *Recall the below set of relations (assuming $\ell_r = r$ for every r):*

$$\mathbf{C}_r = [\mathbf{P}_{r,m_r}^\top, \mathbf{P}_{r+1,m_r}^\top]^\top = [\mathbf{M}_r, \mathbf{M}_{r+1}]^\top \mathbf{B} \mathbf{M}_{m_r}. \quad (59)$$

The top- K SVD of \mathbf{C}_r results in the below relation:

$$\mathbf{C}_r = [\overline{\mathbf{U}}_r^\top, \overline{\mathbf{U}}_{r+1}^\top]^\top \boldsymbol{\Sigma}_r \mathbf{V}_{m_r}^\top. \quad (60)$$

From (59) and (60), we get that there exists a nonsingular matrix $\overline{\mathbf{G}}_r$ such that

$$[\overline{\mathbf{U}}_r^\top, \overline{\mathbf{U}}_{r+1}^\top]^\top = [\mathbf{M}_r, \mathbf{M}_{r+1}]^\top \overline{\mathbf{G}}_r, \quad (61)$$

where the matrix $[\overline{\mathbf{U}}_r^\top, \overline{\mathbf{U}}_{r+1}^\top]^\top$ is semi-orthogonal. We invoke the below fact to proceed further.

Fact 1 *Consider the equation $\overline{\mathbf{U}} = \overline{\mathbf{M}}^\top \overline{\mathbf{G}}$ where the matrix $\overline{\mathbf{U}}$ is tall and is semi-orthogonal. Then the below holds:*

$$\sigma_{\max}(\overline{\mathbf{G}}) = 1/\sigma_{\min}(\overline{\mathbf{M}}) \quad \text{and} \quad \sigma_{\min}(\overline{\mathbf{G}}) = 1/\sigma_{\max}(\overline{\mathbf{M}}).$$

Proof 3 Since $\bar{\mathbf{U}}$ is a semi-orthogonal matrix, we have

$$\begin{aligned}\bar{\mathbf{U}}^\top \bar{\mathbf{U}} &= \mathbf{I}, \\ \implies \bar{\mathbf{G}}^\top \bar{\mathbf{M}} \bar{\mathbf{M}}^\top \bar{\mathbf{G}} &= \mathbf{I}, \\ \implies \bar{\mathbf{M}} \bar{\mathbf{M}}^\top &= \bar{\mathbf{G}}^{-\top} \bar{\mathbf{G}}^{-1} = (\bar{\mathbf{G}} \bar{\mathbf{G}}^\top)^{-1}.\end{aligned}$$

The above relation implies that $\sigma_{\max}(\bar{\mathbf{G}}) = 1/\sigma_{\min}(\bar{\mathbf{M}})$, $\sigma_{\min}(\bar{\mathbf{G}}) = 1/\sigma_{\max}(\bar{\mathbf{M}})$ hold true.

Due to Fact 1, from (61), we get

$$\sigma_{\max}(\bar{\mathbf{G}}_r) = \frac{1}{\sigma_{\min}([\mathbf{M}_r, \mathbf{M}_{r+1}])} \quad \text{and} \quad \sigma_{\min}(\bar{\mathbf{G}}_r) = \frac{1}{\sigma_{\max}([\mathbf{M}_r, \mathbf{M}_{r+1}])}. \quad (62)$$

Next we consider the below relation obtained from (61):

$$\bar{\mathbf{U}}_r = \mathbf{M}_r^\top \bar{\mathbf{G}}_r.$$

Since \mathbf{M}_r is full row-rank, we have

$$\begin{aligned}\sigma_{\min}(\bar{\mathbf{U}}_r) &= \min_{\|\mathbf{x}\|_2=1} \|\mathbf{M}_r^\top \bar{\mathbf{G}}_r \mathbf{x}\|_2 \\ &\geq \min_{\|\mathbf{x}\|_2=1} \sigma_{\min}(\mathbf{M}_r) \|\bar{\mathbf{G}}_r \mathbf{x}\|_2 = \sigma_{\min}(\mathbf{M}_r) \min_{\|\mathbf{x}\|_2=1} \|\bar{\mathbf{G}}_r \mathbf{x}\|_2 \\ &= \sigma_{\min}(\mathbf{M}_r) \sigma_{\min}(\bar{\mathbf{G}}_r) = \frac{\sigma_{\min}(\mathbf{M}_r)}{\sigma_{\max}([\mathbf{M}_r, \mathbf{M}_{r+1}])} \geq \frac{\alpha_{\min}}{\beta_{\max}},\end{aligned}$$

where we have applied (62) to obtain the last equality and used the Assumption 2 and Lemma 3 for the last inequality.

Similarly, we can easily have,

$$\begin{aligned}\sigma_{\max}(\bar{\mathbf{U}}_r) &\leq \sigma_{\max}(\bar{\mathbf{G}}_r) \sigma_{\max}(\mathbf{M}_r) \\ &= \frac{\sigma_{\max}(\mathbf{M}_r)}{\sigma_{\min}([\mathbf{M}_r, \mathbf{M}_{r+1}])} \leq \frac{\alpha_{\max}}{\beta_{\min}}.\end{aligned}$$

Combining Lemma 13 with (58), we have

$$\|\hat{\bar{\mathbf{U}}}_r^\dagger - (\bar{\mathbf{U}}_r \mathbf{O}_r)^\dagger\|_2 \leq \frac{2\sqrt{2}\beta_{\max}^2}{\alpha_{\min}^2} \|\hat{\bar{\mathbf{U}}}_r - (\bar{\mathbf{U}}_r \mathbf{O}_r)\|_2 \quad (63)$$

G Proof of Lemma 5

For simpler notations, let us define $\mathbf{G}_1 := \bar{\mathbf{U}}_{r+1}\mathbf{O}_r$, $\mathbf{G}_2 := (\bar{\mathbf{U}}_r\mathbf{O}_r)^\dagger$ and $\mathbf{G}_3 := \mathbf{U}_r\mathbf{O}$. Also we define $\hat{\mathbf{G}}_1 := \hat{\mathbf{U}}_{r+1}$, $\hat{\mathbf{G}}_2 := (\hat{\mathbf{U}}_r)^\dagger$ and $\mathbf{G}_3 := \hat{\mathbf{U}}_r\mathbf{O}$. With these, consider the below:

$$\begin{aligned}
\left\| \hat{\mathbf{G}}_1 \hat{\mathbf{G}}_2 \hat{\mathbf{G}}_3 - \mathbf{G}_1 \mathbf{G}_2 \mathbf{G}_3 \right\|_2 &= \left\| \hat{\mathbf{G}}_1 \hat{\mathbf{G}}_2 \hat{\mathbf{G}}_3 - \mathbf{G}_1 \mathbf{G}_2 \mathbf{G}_3 - \hat{\mathbf{G}}_1 \mathbf{G}_2 \mathbf{G}_3 + \hat{\mathbf{G}}_1 \mathbf{G}_2 \mathbf{G}_3 \right\|_2 \\
&= \left\| (\hat{\mathbf{G}}_1 - \mathbf{G}_1) \mathbf{G}_2 \mathbf{G}_3 + \hat{\mathbf{G}}_1 (\hat{\mathbf{G}}_2 \hat{\mathbf{G}}_3 - \mathbf{G}_2 \mathbf{G}_3) \right\|_2 \\
&\leq \left\| (\hat{\mathbf{G}}_1 - \mathbf{G}_1) \mathbf{G}_2 \mathbf{G}_3 \right\|_2 + \left\| \hat{\mathbf{G}}_1 (\hat{\mathbf{G}}_2 \hat{\mathbf{G}}_3 - \mathbf{G}_2 \mathbf{G}_3) \right\|_2 \\
&= \left\| (\hat{\mathbf{G}}_1 - \mathbf{G}_1) \mathbf{G}_2 \mathbf{G}_3 \right\|_2 + \left\| \hat{\mathbf{G}}_1 (\hat{\mathbf{G}}_2 - \mathbf{G}_2) \mathbf{G}_3 + \hat{\mathbf{G}}_1 \hat{\mathbf{G}}_2 (\hat{\mathbf{G}}_3 - \mathbf{G}_3) \right\|_2 \\
&\leq \|\mathbf{G}_2\|_2 \|\mathbf{G}_3\|_2 \left\| \hat{\mathbf{G}}_1 - \mathbf{G}_1 \right\|_2 + \|\hat{\mathbf{G}}_1\|_2 \|\mathbf{G}_3\|_2 \left\| \hat{\mathbf{G}}_2 - \mathbf{G}_2 \right\|_2 \\
&\quad + \|\hat{\mathbf{G}}_1\|_2 \|\hat{\mathbf{G}}_2\|_2 \left\| \hat{\mathbf{G}}_3 - \mathbf{G}_3 \right\|_2, \tag{64}
\end{aligned}$$

where we have applied triangle inequality and the fact that $\|\mathbf{AB}\|_2 \leq \|\mathbf{A}\|_2 \|\mathbf{B}\|_2$ to obtain the first and last inequalities, respectively.

We introduce the following lemma and then proceed to characterize $\|\hat{\mathbf{G}}_1\|_2$, $\|\mathbf{G}_2\|_2$, $\|\hat{\mathbf{G}}_2\|_2$ and $\|\mathbf{G}_3\|_2$.

Lemma 14 *Suppose that Assumption 2 holds. Then, we have $\sigma_{\max}(\mathbf{U}_r) \leq \frac{\alpha_{\max}}{\beta_{\min}}$.*

The proof of the lemma is provided in the following section H.

- **Bound for $\|\hat{\mathbf{G}}_1\|_2 = \|\hat{\mathbf{U}}_{r+1}\|_2$**

$$\begin{aligned}
\|\hat{\mathbf{G}}_1\|_2 &= \|\hat{\mathbf{U}}_{r+1}\|_2 \\
&= \|\hat{\mathbf{U}}_{r+1} - \bar{\mathbf{U}}_{r+1}\mathbf{O}_r + \bar{\mathbf{U}}_{r+1}\mathbf{O}_r\|_2 \\
&\leq \|\hat{\mathbf{U}}_{r+1} - \bar{\mathbf{U}}_{r+1}\mathbf{O}_r\|_2 + \|\bar{\mathbf{U}}_{r+1}\mathbf{O}_r\|_2 \\
&\leq \sigma_{\max}(\bar{\mathbf{U}}_{r+1}) + \sigma_{\max}(\bar{\mathbf{U}}_{r+1}) = 2\sigma_{\max}(\bar{\mathbf{U}}_{r+1}) \leq 2\frac{\alpha_{\max}}{\beta_{\min}}.
\end{aligned}$$

where we have used triangle inequality for the first inequality, used the assumption that $\|\hat{\mathbf{U}}_{r+1} - \bar{\mathbf{U}}_{r+1}\mathbf{O}_r\|_2 \leq \sigma_{\min}(\bar{\mathbf{U}}_{r+1})/2$ for the second inequality and invoked Lemma 13 for the last inequality.

- **Bound for $\|\mathbf{G}_2\|_2 = \|(\bar{\mathbf{U}}_r\mathbf{O}_r)^\dagger\|_2$**

$$\|\mathbf{G}_2\|_2 = \|(\bar{\mathbf{U}}_r\mathbf{O}_r)^\dagger\|_2 = 1/\sigma_{\min}(\bar{\mathbf{U}}_r) \leq \frac{\beta_{\max}}{\alpha_{\min}},$$

where we have applied Lemma 13 for the last inequality.

- **Bound for** $\|\widehat{\mathbf{G}}_2\|_2 = \|\widehat{\mathbf{U}}_r^\dagger\|_2$

$$\begin{aligned}\|\widehat{\mathbf{G}}_2\|_2 &= \|\widehat{\mathbf{U}}_r^\dagger\|_2 \\ &= 1/\sigma_{\min}(\widehat{\mathbf{U}}_r) \\ &\leq 2/\sigma_{\min}(\overline{\mathbf{U}}_r) \leq 2\frac{\beta_{\max}}{\alpha_{\min}},\end{aligned}$$

where we have used applied Lemma 12 by using the assumption that $\|\widehat{\mathbf{U}}_r - \overline{\mathbf{U}}_r \mathbf{O}_r\|_2 \leq \sigma_{\min}(\overline{\mathbf{U}}_r)/2$ for the first inequality and invoked Lemma 13 for the last inequality.

- **Bound for** $\|\mathbf{G}_3\|_2 = \|\mathbf{U}_r \mathbf{O}\|_2$

$$\begin{aligned}\|\mathbf{G}_3\|_2 &= \|\mathbf{U}_r \mathbf{O}\|_2 \\ &= \|\mathbf{U}_r\|_2 \leq \frac{\alpha_{\max}}{\beta_{\min}},\end{aligned}$$

where we have invoked Lemma 14 for the inequality.

Applying these upper bounds in (64), we finally have

$$\begin{aligned}\left\|\widehat{\mathbf{G}}_1 \widehat{\mathbf{G}}_2 \widehat{\mathbf{G}}_3 - \mathbf{G}_1 \mathbf{G}_2 \mathbf{G}_3\right\|_2 &\leq \frac{\beta_{\max}}{\alpha_{\min}} \frac{\alpha_{\max}}{\beta_{\min}} \left\|\widehat{\mathbf{G}}_1 - \mathbf{G}_1\right\|_2 + 2\frac{\alpha_{\max}}{\beta_{\min}} \frac{\alpha_{\max}}{\beta_{\min}} \left\|\widehat{\mathbf{G}}_2 - \mathbf{G}_2\right\|_2 \\ &\quad + 4\frac{\beta_{\max}}{\alpha_{\min}} \frac{\alpha_{\max}}{\beta_{\min}} \left\|\widehat{\mathbf{G}}_3 - \mathbf{G}_3\right\|_2.\end{aligned}$$

H Proof of Lemma 14

Proof 4 *Theorem 1 shows that there exists a certain nonsingular \mathbf{G} such that for each true basis \mathbf{U}_r for $r \in [L]$, we have:*

$$\mathbf{U}_r = \mathbf{M}_r^\top \mathbf{G}. \quad (65)$$

Recall that, under noiseless case, Algorithm 1 first directly estimates \mathbf{U}_T and \mathbf{U}_{T+1} by performing the top- K SVD to $\mathbf{C}_T = [\mathbf{P}_{T,m_T}^\top, \mathbf{P}_{T+1,m_T}^\top]^\top$ (assuming $\ell_r = r$ for every r) where

$$\mathbf{C}_T = [\mathbf{U}_T^\top, \mathbf{U}_{T+1}^\top]^\top \boldsymbol{\Sigma}_T \mathbf{V}_{m_T}^\top. \quad (66)$$

The above implies that,

$$[\mathbf{U}_T^\top, \mathbf{U}_{T+1}^\top]^\top = [\mathbf{M}_T, \mathbf{M}_{T+1}]^\top \mathbf{G}$$

holds where $[\mathbf{U}_T^\top, \mathbf{U}_{T+1}^\top]$ is semi-orthogonal. By utilizing Fact 1, we get $\sigma_{\max}(\mathbf{G}) = 1/\sigma_{\min}([\mathbf{M}_T, \mathbf{M}_{T+1}])$ and $\sigma_{\min}(\mathbf{G}) = 1/\sigma_{\max}([\mathbf{M}_T, \mathbf{M}_{T+1}])$. Using this result, from (65), we have

$$\sigma_{\max}(\mathbf{U}_r) \leq \sigma_{\max}(\mathbf{G}) \sigma_{\max}(\mathbf{M}_r) \leq \frac{\sigma_{\max}(\mathbf{M}_r)}{\sigma_{\min}([\mathbf{M}_T, \mathbf{M}_{T+1}])} \leq \frac{\alpha_{\max}}{\beta_{\min}},$$

where we have utilized Assumption 2 and Lemma 3 to obtain the last inequality.

I Proof of Lemma 6

Let us first consider the below:

$$\mathbf{C}_r = [\mathbf{P}_{\ell_r, m_r}^\top, \mathbf{P}_{\ell_{r+1}, m_r}^\top]^\top = [\mathbf{M}_{\ell_r}, \mathbf{M}_{\ell_{r+1}}]^\top \mathbf{B} \mathbf{M}_{m_r}.$$

Consider the K -th eigenvalue of the symmetric matrix $\mathbf{C}_r^\top \mathbf{C}_r$:

$$\lambda_K(\mathbf{C}_r^\top \mathbf{C}_r) = \lambda_K(\underbrace{\mathbf{M}_{m_r}^\top \mathbf{B} [\mathbf{M}_{\ell_r}, \mathbf{M}_{\ell_{r+1}}] [\mathbf{M}_{\ell_r}, \mathbf{M}_{\ell_{r+1}}]^\top}_{\mathbf{W}_1 \in \mathbb{R}^{N/L \times K}} \underbrace{\mathbf{B} \mathbf{M}_{m_r}}_{\mathbf{W}_2 \in \mathbb{R}^{K \times N/L}}), \quad (67)$$

where λ_K denotes the K th eigenvalue with $\lambda_1 \geq \dots \geq \lambda_K$.

We utilize the below fact to proceed further:

Lemma 15 (Theorem 1.3.22) [46] *Consider two matrices $\mathbf{W}_1 \in \mathbb{R}^{N \times K}$ and $\mathbf{W}_2 \in \mathbb{R}^{K \times N}$. Let $\lambda_1, \dots, \lambda_K$ be the nonzero eigenvalues of the matrix $\mathbf{W}_1 \mathbf{W}_2$. Then, the matrix $\mathbf{W}_2 \mathbf{W}_1$ also holds the same set of eigenvalues.*

Combining Lemma 15 and (67), we have

$$\lambda_K(\mathbf{C}_r^\top \mathbf{C}_r) = \lambda_K(\mathbf{B} \mathbf{M}_{m_r} \mathbf{M}_{m_r}^\top \mathbf{B} [\mathbf{M}_{\ell_r}, \mathbf{M}_{\ell_{r+1}}] [\mathbf{M}_{\ell_r}, \mathbf{M}_{\ell_{r+1}}]^\top). \quad (68)$$

Next, we consider the following matrix

$$\mathbf{H}_r := \mathbf{M}_{m_r} \mathbf{M}_{m_r}^\top = \sum_{n=1}^{N/L} \mathbf{M}_{m_r}(:, n) \mathbf{M}_{m_r}(:, n)^\top. \quad (69)$$

To proceed, we have the lemma from [27] to bound $\lambda_K(\mathbf{H}_r)$ and $\lambda_1(\mathbf{H}_r)$.

Lemma 16 [27] *Assume that the columns of \mathbf{M} are generated from any continuous distribution. Then, there exists positive constants c and C depending only on distribution of the columns of \mathbf{M} such that*

$$\begin{aligned} \Pr(\lambda_K(\mathbf{H}_r) \leq c(N/L)) &\leq K \exp(-c(N/4L)), \\ \Pr(\lambda_1(\mathbf{H}_r) \geq C(N/L)) &\leq \frac{K}{2^{CN/L}}. \end{aligned}$$

To simplify the bound on the probability, let us find the conditions at which the following is satisfied:

$$K \exp(-c(N/4L)) \leq (N/L)^{-1}, \quad (70)$$

$$\frac{K}{2^{CN/L}} \leq (N/L)^{-1}. \quad (71)$$

The conditions (70) and (71) are equivalent to the following:

$$(N/L) \geq \frac{4}{c} \log(NK/L), \quad (72)$$

$$(N/L) \geq \frac{\log_2 e}{C} \log(NK/L). \quad (73)$$

We can immediately see that if (72) is satisfied, (73) is also satisfied since $c \leq C$.

Therefore, we get that if $(N/L) \geq \frac{4}{c} \log(NK/L)$, with probability atleast $1 - (N/L)^{-1}$,

$$\lambda_K(\mathbf{M}_{m_r} \mathbf{M}_{m_r}^\top) \leq c(N/L), \quad (74a)$$

$$\lambda_1(\mathbf{M}_{m_r} \mathbf{M}_{m_r}^\top) \geq C(N/L). \quad (74b)$$

Using the above result, we can also have

$$\lambda_K([\mathbf{M}_{\ell_r}, \mathbf{M}_{\ell_{r+1}}][\mathbf{M}_{\ell_r}, \mathbf{M}_{\ell_{r+1}}]^\top) \geq c(2N/L), \quad (75a)$$

$$\lambda_1([\mathbf{M}_{\ell_r}, \mathbf{M}_{\ell_{r+1}}][\mathbf{M}_{\ell_r}, \mathbf{M}_{\ell_{r+1}}]^\top) \leq C(2N/L), \quad (75b)$$

each holding with probability at least $1 - (2N/L)^{-1}$.

Thus, applying (74) and (75) in (68), we get

$$\begin{aligned} \lambda_K(\mathbf{C}_r^\top \mathbf{C}_r) &\geq \lambda_K^2(\mathbf{B}) \lambda_K([\mathbf{M}_{\ell_r}, \mathbf{M}_{\ell_{r+1}}][\mathbf{M}_{\ell_r}, \mathbf{M}_{\ell_{r+1}}]^\top) \lambda_K(\mathbf{M}_{m_r} \mathbf{M}_{m_r}^\top) \\ &\geq \lambda_K^2(\mathbf{B}) c(2N/L) c(N/L) = 2\lambda_K^2(\mathbf{B}) c^2(N/L)^2, \\ &= 2\sigma_{\min}^2(\mathbf{B}) c^2(N/L)^2, \end{aligned}$$

with probability at least $1 - (2N/3L)^{-1}$ where we have used the facts that $\lambda_1((\mathbf{A}\mathbf{B})^{-1}) \leq \lambda_1(\mathbf{A}^{-1})\lambda_1(\mathbf{B}^{-1})$ and $\lambda_1(\mathbf{A}^{-1}) = 1/\lambda_K(\mathbf{A})$ for obtaining the first inequality and used $\lambda_K(\mathbf{B}) = \sigma_{\min}(\mathbf{B})$ for the last equality.

Similarly, we can get the below with probability at least $1 - (2N/3L)^{-1}$:

$$\begin{aligned} \lambda_1(\mathbf{C}_r^\top \mathbf{C}_r) &\leq \lambda_1^2(\mathbf{B}) \lambda_1([\mathbf{M}_{\ell_r}, \mathbf{M}_{\ell_{r+1}}][\mathbf{M}_{\ell_r}, \mathbf{M}_{\ell_{r+1}}]^\top) \lambda_1(\mathbf{M}_{m_r} \mathbf{M}_{m_r}^\top) \\ &\leq \lambda_1^2(\mathbf{B}) C(2N/L) C(N/L) = 2\lambda_1^2(\mathbf{B}) C^2(N/L)^2, \\ &= 2\sigma_{\max}^2(\mathbf{B}) C^2(N/L)^2. \end{aligned}$$

Therefore, by taking union bound over every $r \in [L-1]$, with probability atleast $1 - (3L(L-1)/N)$, the following equations hold simultaneously for every r :

$$\sigma_{\min}([\mathbf{P}_{\ell_r, m_r}^\top, \mathbf{P}_{\ell_{r+1}, m_r}^\top]^\top) = \sigma_{\min}(\mathbf{C}_r) = \sqrt{\lambda_K(\mathbf{C}_r^\top \mathbf{C}_r)} \geq \sqrt{2}\sigma_{\min}(\mathbf{B})c(N/L), \quad (76)$$

$$\sigma_{\max}([\mathbf{P}_{\ell_r, m_r}^\top, \mathbf{P}_{\ell_{r+1}, m_r}^\top]^\top) = \sigma_{\max}(\mathbf{C}_r) = \sqrt{\lambda_1(\mathbf{C}_r^\top \mathbf{C}_r)} \leq \sqrt{2}\sigma_{\max}(\mathbf{B})C(N/L). \quad (77)$$

The equations (76) and (77) immediately follow that the below holds with probability atleast $1 - (3L(L-1)/N)$ if the condition (70) holds true :

$$\begin{aligned} \sigma_K &= \min_{r \in \{1, \dots, L-1\}} \sigma_{\min}([\mathbf{P}_{\ell_r, m_r}^\top, \mathbf{P}_{\ell_{r+1}, m_r}^\top]^\top) \geq \sqrt{2}\sigma_{\min}(\mathbf{B})c(N/L), \\ \sigma_1 &= \max_{r \in \{1, \dots, L-1\}} \sigma_{\max}([\mathbf{P}_{\ell_r, m_r}^\top, \mathbf{P}_{\ell_{r+1}, m_r}^\top]^\top) \leq \sqrt{2}\sigma_{\max}(\mathbf{B})C(N/L). \end{aligned}$$

J Proof of Lemma 8

We consider the given noisy NMF model:

$$\hat{\mathbf{U}}^\top = \mathbf{O}^\top \mathbf{G}^\top \mathbf{M} + \mathbf{N}.$$

It is given that there exists a set of indices $\Delta := \{n_1, \dots, n_K\}$ such that $\mathbf{M}(:, \Delta) = \mathbf{I}_K + \mathbf{E}$, where $\mathbf{E} \in \mathbb{R}^{K \times K}$ is the error matrix with $\|\mathbf{E}(:, k)\|_2 \leq \varepsilon$ and \mathbf{I}_K is the identity matrix of size $K \times K$. Without loss of generality, we let $\Delta = \{1, \dots, K\}$. Therefore, we have

$$\begin{aligned}\widehat{\mathbf{U}}^\top &= \mathbf{O}^\top \mathbf{G}^\top \mathbf{M} + \mathbf{N} = \mathbf{O}^\top \mathbf{G}^\top [\mathbf{I}_K + \mathbf{E}, \widetilde{\mathbf{M}}] + \mathbf{N} \\ &= \mathbf{O}^\top \mathbf{G}^\top [\mathbf{I}_K, \widetilde{\mathbf{M}}] + [\mathbf{O}^\top \mathbf{G}^\top \mathbf{E}, \mathbf{0}] + \mathbf{N},\end{aligned}$$

where the zero matrix $\mathbf{0}$ has the same dimension of $\widetilde{\mathbf{M}}$.

Let $\widetilde{\mathbf{N}} = [\mathbf{O}^\top \mathbf{G}^\top \mathbf{E}, \mathbf{0}] + \mathbf{N}$. This gives us the noisy NMF model as

$$\widehat{\mathbf{U}}^\top = \underbrace{\mathbf{O}^\top \mathbf{G}^\top}_{\mathbf{W}} \underbrace{[\mathbf{I}_K, \widetilde{\mathbf{M}}]}_{\mathbf{M}} + \widetilde{\mathbf{N}}. \quad (78)$$

Then, the below holds for any $k \in [K]$:

$$\begin{aligned}\|\widetilde{\mathbf{N}}(:, k)\|_2 &\leq \|\mathbf{G}\mathbf{O}\|_2 \|\mathbf{E}(:, k)\|_2 + \|\mathbf{N}(:, k)\|_2, \\ &\leq \sigma_{\max}(\mathbf{G})\varepsilon + \zeta := \widetilde{\zeta}(\mathbf{G}),\end{aligned} \quad (79)$$

where the first inequality is by applying triangle inequality and the second inequality is by using the orthogonality of \mathbf{O} and also by using the given assumption $\|\mathbf{N}(:, k)\|_2 \leq \zeta$.

We utilize the below lemma from [33] which characterizes the estimation accuracy of SPA under the NMF model (78).

Lemma 17 [33] *Consider the noisy model in (78) and suppose that \mathbf{W} is full rank and \mathbf{M} satisfies the simplex constraints, i.e., $\mathbf{M} \geq \mathbf{0}, \mathbf{1}^\top \mathbf{M} = \mathbf{1}^\top$. Let each column of $\widetilde{\mathbf{N}}$ satisfies the condition $\|\widetilde{\mathbf{N}}(:, k)\|_2 \leq \widetilde{\zeta}$ with*

$$\widetilde{\zeta} \leq \sigma_{\min}(\mathbf{W}) \varrho \widetilde{\kappa}^{-1}(\mathbf{W}). \quad (80)$$

Then the SPA Algorithm returns indices $\widehat{\Delta} = \{\hat{n}_1, \dots, \hat{n}_K\}$ such that for each k ,

$$\min_{\pi} \|\widehat{\mathbf{U}}(\hat{n}_k, :) - \mathbf{W}(:, \pi(k))\|_2 \leq \widetilde{\kappa}(\mathbf{W}) \widetilde{\zeta}, \quad (81)$$

where $\widetilde{\kappa}(\mathbf{W}) := 1 + 80\kappa^2(\mathbf{W})$, $\varrho := \min\left(\frac{1}{2\sqrt{K-1}}, \frac{1}{4}\right)$ and π is certain permutation for $k \in [K]$.

Therefore, we can apply Lemma 17 to the the noisy model in (78) and obtain an estimate $\widehat{\mathbf{G}} = \widehat{\mathbf{U}}(\widehat{\Delta}, :)$ by applying SPA such that

$$\|\widehat{\mathbf{G}} - \mathbf{\Pi} \mathbf{G} \mathbf{O}\|_{\text{F}} \leq \sqrt{K} \widetilde{\kappa}(\mathbf{G}) \widetilde{\zeta}(\mathbf{G}). \quad (82)$$

In the above, we applied $\mathbf{W} = \mathbf{O}^\top \mathbf{G}^\top$, used the norm equivalence to convert from ℓ_2 -norm to the Frobenius norm, used the fact that $\sigma_{\min}(\mathbf{G}\mathbf{O}) = \sigma_{\min}(\mathbf{G})$ and $\sigma_{\max}(\mathbf{G}\mathbf{O}) = \sigma_{\max}(\mathbf{G})$ due to the orthogonality of the matrix \mathbf{O} and $\mathbf{\Pi}$ is a permutation matrix such that $\mathbf{\Pi} = \arg \min_{\mathbf{\Pi}} \|\widehat{\mathbf{G}} - \mathbf{\Pi} \mathbf{G} \mathbf{O}\|_{\text{F}}$.

Also, the condition in Lemma 17 can be represented as

$$\widetilde{\zeta}(\mathbf{G}) = \sigma_{\max}(\mathbf{G})\varepsilon + \zeta \leq \frac{\sigma_{\min}(\mathbf{G})\varrho}{\widetilde{\kappa}(\mathbf{G})}. \quad (83)$$

Next, we proceed to characterize the singular values of \mathbf{G} to express the above bound in more intuitive way. To this end, we have the following lemma:

Lemma 18 *Under Assumption 2, the below relations hold:*

$$\begin{aligned}\sigma_{\max}(\mathbf{G}) &= 1/\sigma_{\min}([\mathbf{M}_T, \mathbf{M}_{T+1}]) \leq 1/\alpha_{\min}, \\ \sigma_{\max}(\mathbf{G}) &\geq \sigma_{\min}(\mathbf{G}) = 1/\sigma_{\max}([\mathbf{M}_T, \mathbf{M}_{T+1}]) \geq 1/(\sqrt{2K}\alpha_{\max}), \\ \kappa(\mathbf{G}) &\leq \sqrt{2K}\gamma.\end{aligned}$$

Proof 5 *Recall that, under noiseless case, Algorithm 1 first directly estimates \mathbf{U}_T and \mathbf{U}_{T+1} by performing the top- K SVD to $\mathbf{C}_T = [\mathbf{P}_{T,m_T}^\top, \mathbf{P}_{T+1,m_T}^\top]^\top$ where*

$$\mathbf{C}_T = [\mathbf{U}_T^\top, \mathbf{U}_{T+1}^\top]^\top \Sigma_T \mathbf{V}_{m_T}^\top. \quad (84)$$

The above relation implies that, $[\mathbf{U}_T^\top, \mathbf{U}_{T+1}^\top]^\top = [\mathbf{M}_T, \mathbf{M}_{T+1}]^\top \mathbf{G}$ holds where $[\mathbf{U}_T^\top, \mathbf{U}_{T+1}^\top]^\top$ is semi-orthogonal.

Applying Fact 1, we can obtain

$$\sigma_{\max}(\mathbf{G}) = 1/\sigma_{\min}([\mathbf{M}_T, \mathbf{M}_{T+1}]) \quad \text{and} \quad \sigma_{\min}(\mathbf{G}) = 1/\sigma_{\max}([\mathbf{M}_T, \mathbf{M}_{T+1}]).$$

Utilizing Assumption 2 on the above, we can further have

$$\sigma_{\max}(\mathbf{G}) \leq 1/\beta_{\min} \quad \text{and} \quad \sigma_{\min}(\mathbf{G}) \geq 1/\beta_{\max}.$$

By applying Lemma 3, we can finally get

$$\sigma_{\max}(\mathbf{G}) \leq 1/\alpha_{\min}, \quad \sigma_{\min}(\mathbf{G}) \geq 1/(\sqrt{2K}\alpha_{\max}) \quad \text{and} \quad \kappa(\mathbf{G}) \leq \sqrt{2K}\gamma.$$

Applying Lemma 18, we have

$$\begin{aligned}\tilde{\kappa}(\mathbf{G}) &= 1 + 80\kappa^2(\mathbf{G}) \leq 1 + 160K\gamma^2 := \tilde{\kappa}(\mathbf{M}), \\ \tilde{\zeta}(\mathbf{G}) &= \sigma_{\max}(\mathbf{G})\varepsilon + \zeta \leq \frac{\varepsilon}{\alpha_{\min}} + \zeta.\end{aligned}$$

Hence the bound in (82) can be written as

$$\|\widehat{\mathbf{G}} - \Pi \mathbf{G} \mathbf{O}\|_F \leq \sqrt{K}\tilde{\kappa}(\mathbf{M})(\varepsilon/\alpha_{\min} + \zeta), \quad (85)$$

and the condition (83) can be rewritten as:

$$\frac{\varepsilon}{\alpha_{\min}} + \zeta \leq \frac{\varrho}{\sqrt{2K}\alpha_{\max}\tilde{\kappa}(\mathbf{M})}. \quad (86)$$

Using the given assumptions on ε and ζ , we can see that (86) gets satisfied.

Now that we have \mathbf{G} estimated as given by (85), the next step is to estimate the matrix \mathbf{M} . Algorithm 1 estimates \mathbf{M} via least squares. To characterize this step, we consider the following lemma:

Lemma 19 [45] *Consider the noiseless model $\mathbf{X} = \mathbf{W}\mathbf{H}$. Suppose that $\widehat{\mathbf{X}}$ and $\widehat{\mathbf{W}}$ are the noisy estimates of \mathbf{X} and \mathbf{W} , respectively. Assume that there exist constants $\phi_1, \phi_2 > 0$ such that $\|\widehat{\mathbf{W}} - \mathbf{W}\|_2 \leq \phi_1\|\mathbf{W}\|_2$, $\|\widehat{\mathbf{X}} - \mathbf{X}\|_2 \leq \phi_2\|\mathbf{X}\|_2$ and $\phi_1\kappa(\mathbf{W}) < 1$. Then we have*

$$\frac{\|\widehat{\mathbf{H}} - \mathbf{H}\|_2}{\|\mathbf{H}\|_2} \leq \frac{\kappa(\mathbf{W})(\phi_1 + \phi_2)}{1 - \phi_1\kappa(\mathbf{W})} + \kappa(\mathbf{W})\phi_1,$$

where $\widehat{\mathbf{H}}$ is the least squares solution to the problem $\widehat{\mathbf{X}} = \widehat{\mathbf{W}}\mathbf{H}$.

By fixing $\mathbf{X} := \mathbf{O}^\top \mathbf{U}^\top$, $\mathbf{W} := \mathbf{O}^\top \mathbf{G}^\top \mathbf{\Pi}^\top$ and $\mathbf{H} := \mathbf{\Pi} \mathbf{M}$, we can apply Lemma 19. By applying the matrix norm equivalence and considering the fact that the matrix \mathbf{O} is orthogonal, the constants ϕ_1 and ϕ_2 in Lemma 19 takes the following values:

$$\phi_1 = \sqrt{K} \tilde{\kappa}(\mathbf{M})(\varepsilon/\alpha_{\min} + \zeta)/\sigma_{\max}(\mathbf{G}), \quad \phi_2 = \zeta/\sigma_{\max}(\mathbf{U}),$$

where the first equality is from (85), the second equality is by using the given assumption that $\|\widehat{\mathbf{U}} - \mathbf{U}\mathbf{O}\|_F = \|\mathbf{N}\|_F \leq \zeta$, and $\tilde{\kappa}(\mathbf{M}) = 1 + 160\gamma^2$.

Then, by applying Lemma 19, the estimation bound for \mathbf{M} can be expressed as

$$\frac{\|\widehat{\mathbf{M}} - \mathbf{\Pi} \mathbf{M}\|_2}{\|\mathbf{M}\|_2} \leq \frac{\kappa(\mathbf{G})(\phi_1 + \phi_2)}{1 - \phi_1 \kappa(\mathbf{G})} + \kappa(\mathbf{G})\phi_1. \quad (87)$$

Using the given assumptions on ε and ζ , we can see that the denominator term $1 - \phi_1 \kappa(\mathbf{G})$ is lower bounded:

$$\begin{aligned} 1 - \phi_1 \kappa(\mathbf{G}) &= 1 - \left(\frac{\sqrt{K} \tilde{\kappa}(\mathbf{M}) \kappa(\mathbf{G})(\varepsilon/\alpha_{\min} + \zeta)}{\sigma_{\max}(\mathbf{G})} \right), \\ &= 1 - \left(\frac{\sqrt{K} \tilde{\kappa}(\mathbf{M})(\varepsilon/\alpha_{\min} + \zeta)}{\sigma_{\min}(\mathbf{G})} \right) \\ &\geq 1 - \left(\sqrt{2} K \alpha_{\max} \tilde{\kappa}(\mathbf{M})(\varepsilon/\alpha_{\min} + \zeta) \right) \geq 1/2. \end{aligned} \quad (88)$$

where we have used the assumptions on ε and ζ for the last inequality. Note the result in (88) also makes sure that the condition $\phi_1 \kappa(\mathbf{G}) < 1$ in Lemma 19 is satisfied.

By applying (88) in the bound (87), we get

$$\begin{aligned} \frac{\|\widehat{\mathbf{M}} - \mathbf{\Pi} \mathbf{M}\|_2}{\|\mathbf{M}\|_2} &\leq 2\kappa(\mathbf{G})(\phi_1 + \phi_2) + \kappa(\mathbf{G})\phi_1 = \kappa(\mathbf{G})(3\phi_1 + 2\phi_2) \\ &= \kappa(\mathbf{G}) \left(\frac{3\sqrt{K} \tilde{\kappa}(\mathbf{M})(\varepsilon/\alpha_{\min} + \zeta)}{\sigma_{\max}(\mathbf{G})} + \frac{2\zeta}{\sigma_{\max}(\mathbf{U})} \right). \end{aligned} \quad (89)$$

Consider the below to lower bound $\sigma_{\max}(\mathbf{U})$ where $\mathbf{U}^\top = \mathbf{G}^\top \mathbf{M}$:

$$\begin{aligned} \sigma_{\max}(\mathbf{U}) &\geq \sigma_{\min}(\mathbf{G})\sigma_{\max}(\mathbf{M}) \\ &= \frac{\sigma_{\max}(\mathbf{M})}{\sigma_{\max}([\mathbf{M}_T, \mathbf{M}_{T+1}])} \geq 1, \end{aligned} \quad (90)$$

where we used Lemma 18 to obtain the first equality and used the fact that $\sigma_{\max}(\mathbf{M}) \geq \sigma_{\max}([\mathbf{M}_T, \mathbf{M}_{T+1}])$ for the last inequality.

Applying Lemma 18 and (90), we have

$$\begin{aligned} \|\widehat{\mathbf{M}} - \mathbf{\Pi} \mathbf{M}\|_2 &\leq \sigma_{\max}(\mathbf{M}) \left(3\sqrt{K} \tilde{\kappa}(\mathbf{M}) \left(\frac{\varepsilon}{\alpha_{\min}} + \zeta \right) \sqrt{2K} \alpha_{\max} + 2\sqrt{2K} \gamma \zeta \right) \\ &= \sigma_{\max}(\mathbf{M}) \left(3\sqrt{2K} \tilde{\kappa}(\mathbf{M}) \gamma \varepsilon + 3\sqrt{2K} \tilde{\kappa}(\mathbf{M}) \alpha_{\max} \zeta + 2\sqrt{2K} \gamma \zeta \right) \\ &\leq \sigma_{\max}(\mathbf{M}) \left(3\sqrt{2K} \tilde{\kappa}(\mathbf{M}) \gamma \varepsilon + 4\sqrt{2K} \tilde{\kappa}(\mathbf{M}) \gamma \zeta \right) \\ &= \sigma_{\max}(\mathbf{M}) \sqrt{2K} \gamma \tilde{\kappa}(\mathbf{M}) (3\varepsilon + 4\zeta), \end{aligned}$$

where $\tilde{\kappa}(\mathbf{M}) = 1 + 160K\gamma^2$.

K Permutation Fixing Procedure for Baseline Algorithms

For synthetic and real data experiments, we employ the procedure in Algorithm 3 for the baseline algorithms to align the permutations of the estimated $\widehat{\mathbf{M}}_\ell$ over different blocks. In Algorithm 3, `BaselineAlgorithm` can be any graph clustering algorithm, for e.g., `GeoNMF`, `CD-MVSI`, `CD-BNMF`, `SC (unnorm.)`, `SC (norm.)`, `k-means` etc.

Algorithm 3 Permutation Fixing Procedure

Require: $\{\mathbf{A}_{\ell,\ell}\}_{\ell=1}^L$, $\{\mathbf{A}_{\ell,\ell+1}\}_{\ell=1}^{L-1}$, K , L , `BaselineAlgorithm`.

```

1:  $\mathbf{\Pi} \leftarrow \mathbf{I}_K$ ;
2: for  $\ell = 1$  to  $L - 1$  do
3:    $\mathbf{H}_\ell \leftarrow \begin{bmatrix} \mathbf{A}_{\ell,\ell} & \mathbf{A}_{\ell,\ell+1} \\ \mathbf{A}_{\ell,\ell+1}^\top & \mathbf{A}_{\ell+1,\ell+1} \end{bmatrix}$ ;
4:    $[\overline{\mathbf{M}}_\ell, \overline{\mathbf{M}}_{\ell+1}] \leftarrow \text{BaselineAlgorithm}(\mathbf{H}_\ell, K)$ ;
5:   if  $\ell > 1$  then
6:      $\mathbf{\Pi} \leftarrow \text{HugarianAlgorithm}(\overline{\mathbf{M}}_\ell, \mathbf{M}_\ell^{(prev)})$  [47];
7:   end if
8:    $[\mathbf{M}_\ell, \mathbf{M}_{\ell+1}] \leftarrow \mathbf{\Pi}^\top [\overline{\mathbf{M}}_\ell, \overline{\mathbf{M}}_{\ell+1}]$ ;
9:    $\mathbf{M}_\ell^{(prev)} \leftarrow \mathbf{M}_{\ell+1}$ ;
10: end for
11:  $\widehat{\mathbf{M}} = [\mathbf{M}_1, \dots, \mathbf{M}_L]$ ;
12: return  $\widehat{\mathbf{M}}$ .

```
